

Localization in Lattice QCD

Maarten Golterman^a and Yigal Shamir^b

^a*Department of Physics and Astronomy, San Francisco State University
San Francisco, CA 94132, USA
maarten@quark.sfsu.edu*

^b*School of Physics and Astronomy
Raymond and Beverly Sackler Faculty of Exact Sciences
Tel-Aviv University, Ramat Aviv, 69978 ISRAEL
shamir@post.tau.ac.il*

ABSTRACT

In this paper, we examine the phase diagram of quenched QCD with two flavors of Wilson fermions, proposing the following microscopic picture. The super-critical regions inside *and* outside the Aoki phase are characterized by the existence of a density of near-zero modes of the (hermitian) Wilson–Dirac operator, and thus by a non-vanishing pion condensate. Inside the Aoki phase, this density is built up from extended near-zero modes, while outside the Aoki phase, there is a non-vanishing density of exponentially localized near-zero modes, which occur in “exceptional” gauge-field configurations. Nevertheless, no Goldstone excitations appear outside the Aoki phase, and the existence of Goldstone excitations may therefore be used to define the Aoki phase in both the quenched and unquenched theories. We show that the density of localized near-zero modes gives rise to a *divergent* pion two-point function, thus providing an alternative mechanism for satisfying the relevant Ward identity in the presence of a non-zero order parameter. This divergence occurs when we take a “twisted” quark mass to zero, and we conclude that quenched QCD with Wilson fermions is well-defined *only* with a non-vanishing twisted mass. We show that this peculiar behavior of the near-zero-mode density is special to the quenched theory by demonstrating that this density vanishes in the unquenched theory outside the Aoki phase. We discuss the implications for domain-wall and overlap fermions constructed from a Wilson–Dirac kernel. We argue that both methods work outside the Aoki phase, but fail inside because of problems with locality and/or chiral symmetry, in both the quenched and unquenched theories.

1. Introduction

Wilson fermions play a prominent role in Lattice QCD [1]. They (and their improved versions) are widely used in numerical calculations of hadronic quantities. In addition, they are at the heart of the construction of lattice Dirac operators with domain-wall [2, 3] or overlap [4, 5] fermions. All these fermion methods based on the Wilson–Dirac operator preserve all of the flavor symmetry, but not ordinary chiral symmetry. For Wilson fermions, a tuning of the bare fermion masses is needed to restore chiral symmetry in the continuum limit, while domain-wall fermions (with infinite extent in the fifth dimension) and overlap fermions possess a modified version of chiral symmetry with essentially the same algebraic properties as the chiral symmetry of the continuum theory [6]. This lattice chiral symmetry reduces to that of the continuum theory in the continuum limit.

In this paper, we will discuss the phase diagram in the gauge-coupling, quark-mass plane for two degenerate Wilson fermions, for both the quenched and unquenched theories. We will be interested in correlation functions constructed from the inverse of the two-flavor (hermitian) Wilson–Dirac operator, evaluated on an equilibrium ensemble of gauge-field configurations. The difference between the quenched and unquenched cases is that only in the unquenched case the fermion determinant (which is positive for two degenerate flavors) will be part of the Boltzmann weight used to generate the ensemble, whereas in the quenched case the Boltzmann weight is obtained from a local pure-gauge action. The quenched theory can be understood as a euclidean path integral with two physical quarks, and two “ghost” (bosonic) quarks with the same mass, whose role it is to cancel the physical-quark determinant [7, 8].

Long ago, a conjecture was made for this phase diagram [9], which is shown schematically in Fig. 1, where g_0 is the bare coupling and m_0 is the bare quark mass. We will be concerned with the region $-8 \leq am_0 \leq 0$ because only in that region can the Wilson–Dirac operator have any zero or near-zero eigenvalues. Spontaneous symmetry breaking (SSB) occurs as a consequence of a non-zero density of such modes [10], and the interesting part of the phase diagram is thus confined to this region (the “super-critical” region). The usual continuum limit corresponds to the critical point at $g_0 = 0$, $am_0 = 0$. Other continuum limits are obtained for any value of am_0 by taking $g_0 \rightarrow 0$, but generically all quarks stay massive (*i.e.* have a mass of order of the cutoff). Only at $-am_0 = 0, 2, 4, 6, 8$ do massless quarks show up in the continuum limit, respectively 2, 8, 12, 8, 2 of them (in our two-flavor theory). The number of quarks is determined by the number of momenta (or “corners”) in the Brillouin zone where the free Wilson–Dirac operator has a zero.

According to this conjecture, in regions A and C no SSB takes place, while region B, the Aoki phase, is defined by the existence of a pionic condensate, which breaks parity and flavor symmetry.¹ Let us briefly review the evidence for the (unquenched) Aoki phase diagram. First, a simple heuristic argument suggests that a pionic condensate must exist in some part of the phase diagram [9]. Start with some

¹Note that all chiral symmetries are explicitly broken at non-zero lattice spacing, and thus play no role in determining the phase diagram.

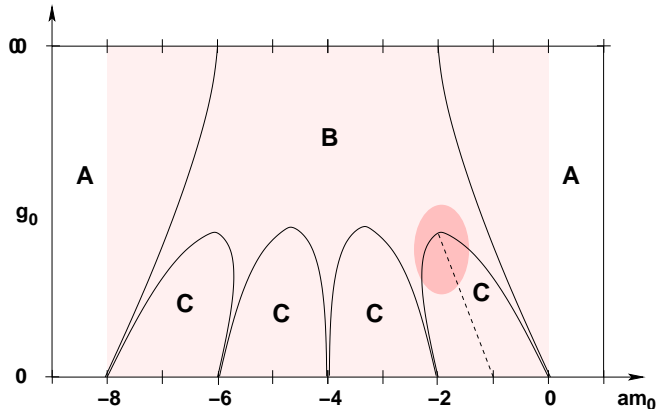


Figure 1: A representation of the phase diagram proposed by Aoki for two-flavor QCD with Wilson fermions and standard plaquette action. The solid lines mark phase transitions (all believed to be continuous). Phase B is the Aoki phase, defined by the existence of a parity- and flavor-breaking pionic condensate. Its “trade mark” are the five “fingers” reaching to the critical points on the $g_0 = 0$ axis. Phases A and C have no condensate. The lightly shaded area marks the super-critical region where near-zero modes may occur. The lines $m_0 = 0$ and $am_0 = -8$, that define the boundaries of the super-critical region, appear to have no special dynamical significance: the A phases extend on both sides of them. The quenched phase diagram is discussed in the main text. The darker shaded area is roughly the area where domain-wall fermion simulations have been carried out. The dashed line represents a possible trajectory for taking the continuum limit with domain-wall or overlap fermions (see Sect. 7).

$m_0 \geq 0$ and examine what happens as m_0 is decreased. For a non-zero lattice spacing a (i.e. $g_0 > 0$) there is no chiral symmetry. Instead of the continuum relation $m_\pi^2 \propto |m_q|$ (here m_π and m_q are respectively the pion and quark masses) we have that $m_\pi^2 \propto m_0 - m'$, where the fact that $m' = m'(g_0)$ does not vanish is a consequence of the breaking of chiral symmetry on the lattice. For $m_0 > m'$ the pions are massive, becoming massless at the critical line $m_0 = m'(g_0)$. For $m_0 < m'$, m_π^2 would go negative, signalling the breaking of a symmetry. A pionic condensate forms in some direction in flavor space, and the line $m_0 = m'(g_0)$ determines the location of a second-order phase transition. The corresponding pion becomes massive again for $m_0 < m'$, while the other two pions become Goldstone bosons associated with the spontaneous breaking of the SU(2) flavor symmetry (“isospin”) down to a U(1) symmetry. Since the condensate is pionic, it breaks parity symmetry as well. Microscopically, the condensate arises from near-zero modes of the Wilson–Dirac operator [10], and can thus only occur in the region $-8 < am_0 < 0$.

This argument does not provide much information on the detailed form of the Aoki phase. Additional analytical evidence comes from several sources. The location of the critical points along the line $g_0 = 0$ is obtained from weak-coupling perturbation

theory, which, however, gives no information on the existence of a condensate. The existence of a condensate was discussed in the context of the pion effective action in Refs. [11, 12]. Ref. [12] showed that, *if* the Aoki phase extends all the way to $g_0 = 0$, it does so as indicated by the “finger” structure² in Fig. 1, with the width of these fingers proportional to $(a\Lambda_{QCD})^3$, where Λ_{QCD} is the QCD scale. In the strong-coupling limit, the location of the two critical points was first found in Ref. [14], and the nature of the phase with broken symmetry was clarified in Ref. [9].

The phase diagram was studied numerically in both quenched [15] and full [16] QCD. The numerical results provide evidence that the five critical points at $g_0 = 0$ are indeed continuously connected to the “main body” of the Aoki phase at large coupling. In the quenched theory, evidence for all ten critical lines at $g_0 = 1$ ($\beta = 6.0$) was found in the last paper of Ref. [15]. In the present paper, in which we address the mechanism responsible for the existence of an Aoki phase, the detailed form of the phase diagram is not important. For the sake of argument, we will assume that the very plausible situation depicted in Fig. 1 describes the actual phase diagram. For a discussion expressing some doubts, see Ref. [17].

A difficulty with the quenched simulations [15] is that exceptional configurations were discarded. Exceptional configurations [18, 19] will play an important role below. Keeping this subtlety in mind, no light excitations were found in the quenched A and C phases, except close to the Aoki (B) phase boundary (and, in particular, close to the five critical points at $g_0 = 0$).

While this picture appears to be rather satisfactory, there exists some evidence that, in the *quenched* case, seems to disagree with the diagram of Fig. 1. Numerical studies of the near-zero modes of the (hermitian) Wilson–Dirac operator indicate that, for $g_0 > 0$, a non-zero density of near-zero modes *always* occurs in the quenched theory, *anywhere* in the super-critical region [20, 21] (namely, in regions B and C, and the super-critical part of region A). Through the Banks–Casher relation, this would imply that the pionic condensate vanishes nowhere in this region, and SSB takes place everywhere, thus contradicting the phase structure sketched in Fig. 1. Moreover, one would be inclined to expect Goldstone excitations everywhere in the super-critical region, in which case Fig. 1 would be completely wrong for the quenched theory; it would not even serve as a guide to the long-range physics. We note however, that this is in conflict with what is known from the numerical studies of Ref. [15] mentioned above, as well as with an analytical study [22], in which it is argued that the effective-field theory analysis of Ref. [12] is also valid for the quenched case.

Another clue comes from a study of a special class of zero modes by Berruto, Narayanan and Neuberger (which we will refer to as BNN hereafter) [23]. They showed that, for choices of m_0 in the super-critical region, the Wilson–Dirac operator has exact zero modes for very smooth gauge fields with one dislocation, which is contained in a small hypercube with a linear size of a few lattice spacings (later we give a more precise description of their results). These zero modes are exponentially localized, and their existence characterizes these “BNN” gauge-field configurations as exceptional configurations. They further argued that in large volume one would

²A similar phase diagram is known to exist in the Gross-Neveu model [9, 13].

expect configurations with a “dilute gas” of such dislocations, because of their highly localized nature. This class of configurations could then contribute to a non-vanishing density of near-zero modes of the Wilson–Dirac operator for the quenched theory, where such configurations are not suppressed by the fermion determinant. This study thus lends analytical support to the numerical results reported in Refs. [20, 21].

In this paper, we will propose a resolution to this apparently paradoxical situation. First, we prove that, if there is a non-vanishing density of exponentially localized near-zero modes, there exists a different mechanism for saturating the Ward identity involving the order parameter for SSB. The orientation of an order parameter is determined by a small external “magnetic field,” here provided by a so-called twisted-mass term [9, 24]. We argue that under the above circumstances, no Goldstone pole need appear, but instead that the two-point function of the would-be Goldstone-pion field *diverges* in the limit of vanishing twisted mass, even if the momentum does *not* vanish.³ This divergence already occurs in finite volume, and we will argue that it persists in the infinite-volume limit of the quenched theory.

We then invoke a concept from condensed-matter physics in order to come up with a conjecture for the microscopic picture underlying the quenched phase diagram. The motivation is to understand what happens in the case that we have a dense, rather than dilute, gas of dislocations. For this purpose, we interpret the square of the hermitian Wilson–Dirac operator as the hamiltonian of a five-dimensional theory, and thus its (positive) eigenvalues as energy eigenvalues. The ensemble of gauge fields on which these eigenvalues are computed act as a random potential, and a non-zero measure subset of these fields can be viewed as random distributions of highly localized scattering centers. The eigenstates describe the possible states of a (four-plus-one-dimensional) “electron” in this background. Note that the fact that we are concerned with the quenched theory here makes the simplicity of this picture more compelling, because of the absence of any feedback of the fermions on the gauge fields.

In general, there will exist a band of extended eigenstates above a certain energy, denoted λ_c^2 , whereas eigenstates below this energy will be localized exponentially.⁴ While attractive-potential scattering centers will tend to localize the electron as in a bound state of an isolated scattering center, a large-enough density of them will make it possible for the electron to travel throughout the lattice by tunneling, with the corresponding state becoming extended. The outcome will depend on the energy of the state and on the density and other properties of the scattering centers. The (average) localization range of the states will increase as the energy is increased towards λ_c^2 , becoming infinite at λ_c^2 , which in condensed-matter physics is referred to as the “mobility edge” [27] (for reviews see Refs. [28, 29, 30]).

The value of the mobility edge is a dynamical issue, which depends on the ensemble of gauge fields, and thus on the location in the phase diagram. We conjecture that the Aoki phase is precisely that region of the phase diagram in which the mobility edge is equal to zero. Outside the Aoki phase, it is larger than zero, and consequently,

³While completing this paper, we became aware of the fact that a similar observation has been made some time ago in condensed matter theory [25].

⁴In a less detailed form, this physical picture has previously been considered in Ref. [26].

all near-zero modes are exponentially localized. When one moves closer to the phase transition, the mobility edge comes down continuously, until it vanishes and the Aoki phase is entered.

We complete our discussion of the physical picture by invoking our results on the two different mechanisms by which the Ward identity can be saturated in the presence of a non-zero condensate. When the mobility edge is zero, only extended near-zero modes contribute to the spectral density, and the Ward identity predicts the existence of Goldstone excitations that dominate the long-range physics of our theory; when the mobility edge is larger than zero, the condensate (and, hence, the order parameter) is produced by exponentially localized near-zero modes, the pion two-point function is diverging, and, we conjecture, no Goldstone excitations occur. Thus the region with Goldstone bosons coincides with the region where the mobility edge is equal to zero, and the existence of Goldstone bosons can be used as a *definition* of the Aoki phase in both unquenched and quenched QCD.

This picture of what the quenched phase diagram looks like begs the question as to whether it is consistent with unquenched QCD. In the unquenched case, the Boltzmann weight is modified by the fermion determinant, which tends to suppress the entropy of gauge-field configurations with near-zero modes. We show that the divergence in the pion two-point function cannot occur in the unquenched case. Therefore, indeed no near-zero-mode density can build up unless the resulting condensate is accompanied by Goldstone bosons (in which case we are inside the Aoki phase), and exponentially localized near-zero modes do not play the same role in unquenched QCD as in quenched QCD.

The scale of the typical localization length of the near-zero modes is set by the lattice spacing. The existence of a non-zero condensate outside the Aoki phase is thus a short-distance artifact. One expects *no* long-range physics (such as the existence of Goldstone excitations) as a consequence of localized near-zero modes, unless their average localization length becomes so large that they behave collectively. According to our conjecture, this happens precisely when the mobility edge comes down to zero, and, just as in unquenched QCD, only extended near-zero modes contribute to the spectral density. Therefore, an effective-lagrangian analysis in terms of the long-range effective degrees of freedom, as carried out in the unquenched case [12], should also make sense in the quenched case. Both inside and close to the boundaries of the Aoki phase, the effective lagrangian should provide a valid description of the long-range physics. Indeed, such an analysis has been carried out in the quenched theory [22], and leads to conclusions very similar to those obtained in the unquenched case.

Thus far, our results deal with the case of QCD with Wilson fermions. However, there are important consequences for lattice QCD with domain-wall or overlap fermions constructed from the Wilson–Dirac operator. In short, we claim that domain-wall and overlap fermions can only be used *well outside* the Aoki phase. For domain-wall fermions, the hermitian Wilson–Dirac operator is closely related to (the logarithm of) the transfer matrix that hops the fermions in the fifth dimension. A density of near-zero modes of the hermitian Wilson–Dirac operator implies the existence of long-range correlations in the fifth direction. This threatens the decoupling of the left-handed and the right-handed quarks that live on opposite ends of the five-

dimensional world, and, hence, the restoration of chiral symmetry in the limit on an infinite fifth dimension.

The crucial issue is the value of the mobility edge of the Wilson–Dirac operator. Well outside the Aoki phase the near-zero modes are all exponentially localized, with a scale set by the lattice spacing. As a result, their contribution to observables vanishes when the four-dimensional separation is set by a physical scale (without having to tune any parameter). As for extended modes of this operator, they cannot mediate long-range correlations in the fifth dimension, and thus they do not obstruct the recovery of chiral symmetry either. In contrast, inside the Aoki phase the near-zero modes are extended, and they mediate long-range correlations in *all* five directions. This strongly suggests that inside the Aoki phase the resulting four-dimensional effective theory either is completely non-local, or, at best, contains long-range degrees of freedom different from the desired ones. This physical picture is valid for any value of the lattice spacing in the fifth dimension a_5 , and thus the same conclusion applies to overlap fermions which corresponds to the special case $a_5 \rightarrow 0$.

This paper is organized as follows. We define our theory, introduce the twisted quark mass, and derive the relevant Ward identity in Sect. 2, where we also briefly review the relation between the condensate and the near-zero-mode density. In Sect. 3 we derive a spectral representation for the pion two-point function. We observe that in the super-critical quenched theory this two-point function always diverges in finite volume, in the limit of a vanishing twisted mass. We thus provide an alternative mechanism for saturating the Ward identity in the presence of a non-vanishing condensate. In Sect. 4, we start with defining localized near-zero modes more precisely. We show that a non-zero density of them will dominate the divergence of the pion two-point function in large volume, and, likely, will produce the divergence in the infinite-volume limit as well. We then give a qualitative but detailed discussion of the mobility edge, and its role in determining which way the Ward identity is satisfied. This leads to a comprehensive picture of the quenched phase diagram, and in particular of the distinction of the super-critical regions inside and outside the Aoki phase. In Sect. 5 we discuss briefly how the picture changes if we reintroduce the fermion determinant, *i.e.* if we unquench the theory. We then discuss the implications of our analysis for domain-wall and overlap fermions in Sect. 6, and finally summarize our conclusions in Sect. 7. In Appendix A we review Anderson’s definition of localization as the (partial) absence of diffusion [27], and its relation to our definition in Sect. 4. Some technical details are relegated to Appendix B.

2. Twisted-mass QCD, the Ward identity, and the Aoki condensate

The definition of the Wilson–Dirac operator is

$$D(m_0) = \frac{1}{a} \begin{pmatrix} -(W + am_0) & C \\ -C^\dagger & -(W + am_0) \end{pmatrix}, \quad (2.1)$$

$$\begin{aligned}
C_{xy} &= \frac{1}{2} \sum_{\mu} \left[\delta_{x+\hat{\mu},y} U_{x\mu} - \delta_{x-\hat{\mu},y} U_{y\mu}^{\dagger} \right] \sigma_{\mu}, \\
W_{xy} &= 4\delta_{xy} - \frac{1}{2} \sum_{\mu} \left[\delta_{x+\hat{\mu},y} U_{x\mu} + \delta_{x-\hat{\mu},y} U_{y\mu}^{\dagger} \right],
\end{aligned}$$

in which $\sigma_{\mu} = (\vec{\sigma}, i)$, where σ_k are the three Pauli matrices, and each entry is a 2×2 matrix. The hermitian Wilson–Dirac operator is $H(m_0) = \gamma_5 D(m_0)$, with $\gamma_5 = \text{diag}(1, 1, -1, -1)$. The theory is symmetric under the replacement $am_0 \rightarrow -(8 + am_0)$ because of the fact that for $am_0 = -4$ the Wilson–Dirac operator only contains nearest-neighbor couplings, thus allowing for a $U(1)_{\epsilon}$ symmetry [18].

We define $H_0(m_0)$ as the operator $H(m_0)$ with all $U_{x\mu} = 1$. This corresponds to the line $g_0 = 0$ in the phase diagram. The spectrum of $H_0^2(m_0)$ covers a closed interval $[(\lambda_{min}^0(m_0))^2, (\lambda_{max}^0(m_0))^2]$, with $0 \leq \lambda_{min}^0(m_0) < \lambda_{max}^0(m_0) < \infty$. λ_{min}^0 is determined by minimizing

$$a^2 H_0^2(p; m_0) = \sum_{\mu} \sin^2(ap_{\mu}) + \left(\sum_{\mu} (1 - \cos(ap_{\mu})) + am_0 \right)^2 \quad (2.2)$$

over the Brillouin zone. Keeping three components of the momentum fixed, it is easy to see that $a^2 H_0^2(p; m_0)$ is linear in the cosine of the fourth component, and thus minimized when this cosine equals ± 1 . It follows that at a minimum all four components of the momenta have to be equal to 0 or π , and thus that $a^2 H_0^2(p; m_0)$ is the minimum over k of $(2k + am_0)^2$, in which k is the number of momentum components equal to π . We thus find that $\lambda_{min}^0 = \min |m_0 - m_0^c|$, where am_0^c is one of the values 0, -2 , -4 , -6 , and -8 . We see that λ_{min}^0 is generically of order $1/a$, except when m_0 is close to one of these critical points. These critical points correspond to the tips of the Aoki “fingers” on the line $g_0 = 0$ in Fig. 1. Near these critical points the theory yields 1, 4, 6, 4, and 1 light quarks per Wilson fermion, respectively. All eigenmodes of $H_0^2(m_0)$ are plane waves, and thus extend over the whole volume. Note that the spectrum of $H_0(m_0)$ is contained in two disjunct intervals, $[-\lambda_{max}^0, -\lambda_{min}^0]$ and $[\lambda_{min}^0, \lambda_{max}^0]$, separated by a gap (if $\lambda_{min}^0 \neq 0$).

Returning to the interacting theory, we consider for which values of m_0 the operator $H(m_0)$, or equivalently $D(m_0)$, can have zero eigenvalues. Write $D(m_0) = A + iB$, with A and B hermitian, and consider an eigenmode $D\Psi = (A + iB)\Psi = \lambda\Psi$. We then have that $\Psi^{\dagger}(A - iB) = \Psi^{\dagger}\lambda^*$, and thus $2\Psi^{\dagger}A\Psi = (\lambda + \lambda^*)\Psi^{\dagger}\Psi$. It follows that λ can only vanish if $\Psi^{\dagger}A\Psi$ vanishes. Since $A = -(W + am_0)$, this can only happen if $-8 \leq am_0 \leq 0$, because the spectrum of W is confined to the interval $[0, 8]$. The super-critical region (*i.e.* the region where zero modes may exist) is thus the region in which $-8 \leq am_0 \leq 0$, and we will restrict ourselves to that region for the rest of this paper.

In the super-critical region “exceptional” configurations may, and do, occur. Exceptional configurations are defined by the condition that $D(m_0)$ has an eigenmode Ψ_0 with an exactly real eigenvalue λ_0 [18, 19]. For such configurations we have that $H(m_0 + \lambda_0)\Psi = \gamma_5 D(m_0 + \lambda_0)\Psi = 0$. Hence, a configuration is exceptional *iff* H has an exact zero mode for some m_0 . BNN configurations (see Sect. 4) are a special kind of exceptional configurations.

We will be interested in a two-flavor theory constructed with this Wilson–Dirac operator, with a fermion lagrangian

$$\begin{aligned}\mathcal{L} &= \bar{\psi}(D(m_0) - im_1\gamma_5\tau_3)\psi \\ &= \bar{\psi}'(H(m_0) - im_1\tau_3)\psi,\end{aligned}\tag{2.3}$$

where $\bar{\psi}' = \bar{\psi}\gamma_5$ is a field redefinition with jacobian one. The (eight-component) field ψ transforms in the fundamental representation of isospin $SU(2)$. We added a symmetry-breaking term proportional to m_1 pointing in the τ_3 direction, where τ_k is another set of Pauli matrices acting in isospin space. This symmetry-breaking term, which breaks both isospin and parity, and thus has the quantum numbers of one of the pions, allows us to probe the existence of an Aoki phase, in which this pion field develops a vacuum expectation value. We will assume the standard plaquette action for the gauge field, unless otherwise noted. Integrating over the fermion fields yields the fermionic partition function

$$Z_F = \prod_n (\lambda_n + im_1)(\lambda_n - im_1) = \prod_n (\lambda_n^2 + m_1^2),\tag{2.4}$$

where the product is over the eigenvalues λ_n of $H(m_0)$, of which there is a finite number on a finite-volume lattice. Note that Z_F depends on the gauge-field configuration through the eigenvalues λ_n .

The relevant Ward identity is obtained by performing a local flavor transformation

$$\delta_+\psi(x) = i\alpha(x)\tau_+\psi(x), \quad \delta_+\bar{\psi}(x) = -i\alpha(x)\bar{\psi}(x)\tau_+,\tag{2.5}$$

in which $\tau_\pm = (\tau_1 \pm i\tau_2)/2$. With $\pi_\pm(x) = i\bar{\psi}(x)\gamma_5\tau_\pm\psi(x)$ and $\pi_3(x) = i\bar{\psi}(x)\gamma_5\tau_3\psi(x)$, we find for any operator \mathcal{O} that

$$\partial_\mu^* \langle J_\mu^+(x) \mathcal{O}(y) \rangle + 2m_1 \langle \pi_+(x) \mathcal{O}(y) \rangle = \frac{i\delta_{xy}}{a^4} \langle \delta_+ \mathcal{O}(y) \rangle,\tag{2.6}$$

where the backward lattice derivative is defined by $\partial_\mu^* f(x) = (f(x) - f(x - \hat{\mu}))/a$ and the corresponding vector current is

$$J_\mu^+(x) = \frac{1}{2} \left(\bar{\psi}(x)\tau_+(\gamma_\mu + 1)U_\mu(x)\psi(x + \hat{\mu}) + \bar{\psi}(x + \hat{\mu})\tau_+(\gamma_\mu - 1)U_\mu^\dagger(x)\psi(x) \right).\tag{2.7}$$

While the notation $\langle \dots \rangle$ indicates an integration over both fermion and gauge fields, we note that the Ward identity is also valid if we integrate over the fermion fields only. Taking $\mathcal{O}(y) = \pi_-(y)$ and defining

$$\begin{aligned}\Gamma(x, y) &= \langle \pi_+(x) \pi_-(y) \rangle, \\ \Gamma_\mu(x, y) &= \langle J_\mu^+(x) \pi_-(y) \rangle,\end{aligned}\tag{2.8}$$

we arrive at the Ward identity

$$\partial_\mu^* \Gamma_\mu(x, y) + 2m_1 \Gamma(x, y) = \frac{\delta_{xy}}{a^4} \langle \pi_3(y) \rangle.\tag{2.9}$$

Defining

$$\tilde{\Gamma}(p) = \frac{a^8}{V} \sum_{xy} e^{ip(y-x)} \Gamma(x, y), \quad (2.10)$$

and similarly $\tilde{\Gamma}_\mu(p)$, the Fourier-transformed Ward identity is

$$\frac{1}{a} \sum_\mu (1 - e^{-iap_\mu}) \tilde{\Gamma}_\mu(p) + 2m_1 \tilde{\Gamma}(p) = \langle \pi_3 \rangle. \quad (2.11)$$

The pionic condensate

$$\langle \pi_3 \rangle = (a^4/V) \sum_y \langle \pi_3(y) \rangle \quad (2.12)$$

can be calculated by first calculating the expectation value of $\pi_3(y)$ in a fixed gauge field (denoted by $\langle \dots \rangle_{\mathcal{U}}$) from Z_F ,

$$a^4 \sum_y \langle \pi_3(y) \rangle_{\mathcal{U}} = Z_F^{-1} \frac{\partial}{\partial m_1} Z_F = 2 \sum_n \frac{m_1}{\lambda_n^2 + m_1^2}, \quad (2.13)$$

and then averaging this over the gauge field, to obtain

$$\langle \pi_3 \rangle = 2 \int d\lambda \rho(\lambda) \frac{m_1}{\lambda^2 + m_1^2}, \quad (2.14)$$

where $\rho(\lambda)$ is the spectral density defined below. In the limit $m_1 \rightarrow 0$, we obtain

$$\langle \pi_3 \rangle = 2\pi\rho(0), \quad (2.15)$$

the Banks–Casher relation [10] for the case at hand.

We define the spectral density from the cumulative density

$$\mathcal{N}(\lambda) = \left\langle \sum_{\lambda_n \leq \lambda} |\Psi_n(x)|^2 \right\rangle, \quad (2.16)$$

where $\Psi_n(x)$ is the eigenfunction associated with the eigenvalue λ_n ,

$$H(m_0)\Psi_n = \lambda_n \Psi_n, \quad (2.17)$$

and with normalization $a^4 \sum_x |\Psi_n(x)|^2 = 1$. Because of the gauge-field average in Eq. (2.16) the right-hand side is actually independent of x . The spectral density $\rho(\lambda)$ is

$$\rho(\lambda) = d\mathcal{N}/d\lambda = V^{-1} \left\langle \sum_n \delta(\lambda - \lambda_n) \right\rangle. \quad (2.18)$$

All these results are valid in finite-volume QCD, in both the quenched and unquenched cases. They remain true if the infinite-volume limit is taken, but of course this limit may or may not commute with the limit $m_1 \rightarrow 0$. It is well known that in unquenched QCD these limits do not commute in a phase with SSB; the order parameter $\langle \pi_3 \rangle$ in the $m_1 = 0$ theory vanishes in finite volume, but does not vanish if the thermodynamic limit is taken before the limit $m_1 \rightarrow 0$. We will return to this point in Sect. 5.

For any given m_0 we will denote by λ_{min}^2 (λ_{max}^2) the minimum (maximum) eigenvalue of $H^2(m_0)$ over the gauge-field space. These values are finite, because of the fact that $H(m_0)$ connects a given site only to a finite number of neighboring sites, and because the gauge group is compact; hence $H(m_0)$ is uniformly bounded. The cumulative density $\mathcal{N}(\lambda)$, defined by the spectrum of $H(m_0)$, is monotonously non-decreasing on the interval $[-\lambda_{max}, \lambda_{max}]$. Using the results of Ref. [23], we will argue below that $\lambda_{min} = 0$ for any $0 > am_0 > -8$ and that, in the quenched theory, $\rho(\lambda) > 0$ for any $-\lambda_{max} < \lambda < \lambda_{max}$. We will first consider a finite volume (Sect. 3) and then the infinite-volume limit (Sect. 4). Outside the super-critical region, *i.e.* for $am_0 > 0$ or $am_0 < -8$, one has $\lambda_{min} > 0$, and $\rho(\lambda) = 0$ for $-\lambda_{min} < \lambda < \lambda_{min}$.

3. Spectral representation of the pion two-point function

We are now ready to establish one of the key results. Using the spectral representation for the quark propagators, it is straightforward to derive that, in a finite volume,

$$\Gamma(x, y) = \int \mathcal{D}\mathcal{U}\mathcal{B}(\mathcal{U}) \sum_{kn} \Psi_n^\dagger(x) \Psi_k(x) \frac{1}{\lambda_k + im_1} \Psi_k^\dagger(y) \Psi_n(y) \frac{1}{\lambda_n - im_1}. \quad (3.1)$$

The two propagators on the right-hand side correspond to the “up” and the “down” quarks respectively. Each sum runs over the eigenstates of the (single-flavor) hermitian Wilson–Dirac operator $H(m_0)$. In full QCD the Boltzmann weight is $\mathcal{B} = Z_F \exp(-S_g)$, where S_g is the gauge action, and the fermionic partition function Z_F is given in Eq. (2.4). In quenched QCD, $\mathcal{B} = \exp(-S_g)$.

For a generic gauge field, the eigenvalue spectrum of $H(m_0)$ is non-degenerate: if $\lambda_n = \lambda_k$ then $\Psi_n(x) = \Psi_k(x)$. Gauge field configurations for which this is not true form a subset of the configuration space with measure zero, because either $H(m_0)$ would have to have a symmetry in this fixed gauge-field background, or there is an accidental degeneracy. Both types of degeneracy disappear under a generic small deformation of the gauge field.

In a finite volume on the lattice, the sums over n and k in Eq. (3.1) are finite, and the integration over gauge fields is absolutely convergent because we integrate over a compact group. This implies that we may interchange the sums and the integral, and consider separately the contribution for each n and k to $\Gamma(x, y)$, which is

$$\int \mathcal{D}\mathcal{U}\mathcal{B}(\mathcal{U}) \Psi_n^\dagger(x) \Psi_k(x) \frac{1}{\lambda_k + im_1} \Psi_k^\dagger(y) \Psi_n(y) \frac{1}{\lambda_n - im_1}. \quad (3.2)$$

For $n \neq k$ (and thus generically $\lambda_n \neq \lambda_k$), expression (3.2) is finite, even in the limit $m_1 \rightarrow 0$. This is because the denominators $\lambda_n + im_1$ and $\lambda_k - im_1$ become singular on different subspaces (with codimension one) of the gauge-field space, and the im_1 terms in the denominators provide an $i\epsilon$ prescription for how to integrate around the poles at $\lambda_n = 0$ or $\lambda_k = 0$. Therefore, in the limit $m_1 \rightarrow 0$ only terms with $n = k$ can make a non-zero contribution to the product $m_1 \Gamma(x, y)$:

$$\lim_{m_1 \rightarrow 0} m_1 \Gamma(x, y) = \lim_{m_1 \rightarrow 0} \int \mathcal{D}\mathcal{U}\mathcal{B}(\mathcal{U}) \sum_n |\Psi_n(x)|^2 |\Psi_n(y)|^2 \frac{m_1}{\lambda_n^2 + m_1^2}. \quad (3.3)$$

Of course, the fact that we keep the volume finite is a key element of this argument. For the Fourier transform of $\Gamma(x, y)$, Eq. (2.10), this result translates into

$$\begin{aligned}\lim_{m_1 \rightarrow 0} m_1 \tilde{\Gamma}(p) &= \lim_{m_1 \rightarrow 0} \frac{m_1}{V} \int \mathcal{D}\mathcal{U} \mathcal{B}(\mathcal{U}) \sum_n \frac{|\mathcal{H}_n(p)|^2}{\lambda_n^2 + m_1^2}, \\ \mathcal{H}_n(p) &= a^4 \sum_x |\Psi_n(x)|^2 e^{-ipx}.\end{aligned}\tag{3.4}$$

Eq. (3.3) has a dramatic consequence for quenched QCD. We may introduce the density correlation function

$$\mathcal{R}(x, y; \lambda) = \int \mathcal{D}\mathcal{U} \mathcal{B}(\mathcal{U}) \sum_n |\Psi_n(x)|^2 |\Psi_n(y)|^2 \delta(\lambda - \lambda_n),\tag{3.5}$$

with which Eq. (3.3) can be written as

$$\lim_{m_1 \rightarrow 0} m_1 \Gamma(x, y) = \lim_{m_1 \rightarrow 0} \int d\lambda \mathcal{R}(x, y; \lambda) \frac{m_1}{\lambda^2 + m_1^2} = \pi \mathcal{R}(x, y; 0).\tag{3.6}$$

It is clear that $\mathcal{R}(x, y; \lambda)$ is independent of m_1 in the quenched theory because $\mathcal{B}(\mathcal{U})$ is. Also, if we choose m_0 anywhere inside the super-critical region, the existence of BNN-like zero modes⁵ implies that there is no spectral gap around $\lambda = 0$, and, in particular, that exact zero modes occur on a non-empty subspace of codimension one. As a result, $\mathcal{R}(x, y; \lambda) > 0$ for any $-\lambda_{max} < \lambda < \lambda_{max}$, because, apart from the delta function, the integrand in Eq. (3.5) is strictly positive. Hence, we find a $1/m_1$ divergence in $\Gamma(x, y)$,

$$\Gamma(x, y) = \frac{\pi \mathcal{R}(x, y; 0)}{m_1} + O(1).\tag{3.7}$$

Moreover, if $\mathcal{R}(x, y; 0) > 0$, also $\rho(0) > 0$ and, from Eq. (2.15), $\langle \pi_3 \rangle > 0$ for the same reasons, and we find that we can have SSB in a *finite* volume in the quenched theory.⁶ Eq. (3.7) shows that the quenched theory in the super-critical region is singular in the limit $m_1 \rightarrow 0$, and it provides an alternative mechanism for saturating the Ward identity Eq. (2.9). With this alternative mechanism, no Goldstone excitations need to appear in the quenched theory, even in the presence of SSB.

The fact that these results are so simple is related to the fact that, in the finite-volume quenched theory, the existence of both the condensate and the $1/m_1$ divergence in the pion two-point function are kinematical effects, which depend only on the super-criticality of m_0 and the strict positivity of the (m_1 -independent) quenched measure. The magnitude of $\langle \pi_3 \rangle > 0$ and $\mathcal{R}(x, y; 0)$ depend on the dynamics, and, as it will turn out, on whether we are inside or outside the Aoki phase.

To conclude this section, we note that one can repeat the entire analysis assuming a different SU(2)-orientation of the flavor- and parity-symmetry breaking term in the lagrangian (2.3). The orientations of both the pionic condensate and the divergent term in the pion two-point function follow the orientation of this symmetry breaking term, just as in the case of conventional SSB. In the next section, we will address the

⁵For a more detailed account of BNN's work, see Sect. 4.

⁶For the unquenched theory, see Sect. 5.

dynamics of the quenched theory, and in the section after that the differences with the unquenched theory.

4. Localization and spontaneous symmetry breaking in the quenched theory

In a given finite volume, all eigenmodes of $H(m_0)$ are localized for the trivial reason that their support is compact. In particular, all near-zero modes contribute to the $1/m_1$ divergence we found in the previous section. (Here we define a near-zero eigenvalue as an eigenvalue with an absolute value of order m_1 , for a given (small) m_1 .) However, as we will now demonstrate, quantitatively the finite-volume divergence comes from exponentially localized near-zero modes. We postpone the discussion of what happens in the infinite-volume limit to the second part of this section.

4.1 Localized modes and the divergence of the pion two-point function

On a finite lattice of spacing a and (large) linear size L (in all four directions), a normalized eigenstate $\Psi_n(x)$ is exponentially localized, provided there exist a positive constant $c_1 = O(1)$, a lattice site x_n^0 (which depends on Ψ_n), and some l with $a \leq l \ll L$ such that

$$|\Psi_n(x)|^2 \leq \frac{c_1}{l^4} \exp\left(-\frac{|x - x_n^0|}{l}\right). \quad (4.1)$$

The *localization range* (or localization length) l_n is the minimal value of l for which the bound (4.1) holds. For definiteness, the distance $|x - y|^2$ is defined by the minimum of $\sum_\mu |x_\mu - y_\mu + n_\mu L|^2$ over all integers n_μ . Our intention is to establish a lower bound on $\tilde{\Gamma}(p)$ in terms of the density of localized near-zero modes and, for this purpose, we take c_1 to be independent of l and L . Also, the restriction to $l_n \leq l \ll L$ means that we consider only localized modes whose support (of roughly order l_n^4), and size $|\Psi_n|^2 \sim 1/l_n^4$ inside this support, are basically independent of the volume. This definition may exclude some modes which would be exponentially localized according to some other reasonable definition, but the class we are considering here will be sufficient for our purpose.

We begin with establishing bounds on $\mathcal{H}_n(p)$ in Eq. (3.4):

$$1 - c_2 l_n^2 p^2 \leq |\mathcal{H}_n(p)|^2 \leq 1. \quad (4.2)$$

Here $c_2 \propto c_1$ is another numerical constant which we will define below. The upper bound is trivial, while the lower bound just expresses the fact that one cannot resolve the structure of a localized mode with localization range l_n using momenta $p \ll 1/l_n$. The lower bound is established by noting that (with x_n^0 the ‘‘center’’ of the localized eigenstate of Eq. (4.1))

$$0 \leq 1 - \text{Re}(e^{ipx_n^0} \mathcal{H}_n(p)) = 2a^4 \sum_x \sin^2(p(x - x_n^0)/2) |\Psi_n(x)|^2 \quad (4.3)$$

$$\begin{aligned}
&\leq \frac{c_1 a^4}{2 l_n^4} \sum_x p^2 (x - x_n^0)^2 e^{-|x - x_n^0|/l_n} \\
&= \frac{\mathcal{C}(l_n)}{2} l_n^2 p^2 \leq \frac{c_2}{2} l_n^2 p^2.
\end{aligned}$$

The inequalities (4.1) and $|\sin(\alpha)| \leq \alpha$ were used. The dimensionless quantity

$$\mathcal{C}(l) = c_1 \frac{a^4}{l^4} \sum_x z^2 e^{-|z|} \Big|_{z_\mu = x_\mu/l} \quad (4.4)$$

is a continuous function of l and finite in the limit $l \rightarrow \infty$. The fact that $\mathcal{C}(l)$ is finite for $l \rightarrow \infty$ is a consequence of choosing the bound on $|\Psi_n(x)|^2$ with the prefactor c_1/l^4 , with c_1 independent of l . This is important for deriving a non-trivial lower bound on $\tilde{\Gamma}(p)$. It thus follows that

$$c_2 \equiv \max_{l \geq a} \{\mathcal{C}(l)\} \quad (4.5)$$

is a finite numerical constant of the same order as c_1 . Since $|\operatorname{Re}(e^{ipx_n^0} \mathcal{H}_n(p))| \leq |\mathcal{H}_n(p)|$ the inequality (4.2) follows.

We now use this bound to derive a lower bound on $\tilde{\Gamma}(p)$ in Eq. (3.4), for $m_1 \rightarrow 0$. Choosing some fixed l , we split the eigenstates of $H(m_0)$ into two classes: those which are exponentially localized according to our definition of Eq. (4.1) with localization range $l_n \leq l$, and the rest. Keeping only the former, we obtain

$$m_1 \tilde{\Gamma}(p) \geq \frac{m_1}{V} \int \mathcal{DUB}(\mathcal{U}) \sum_{l_n \leq l} \frac{1 - c_2 l_n^2 p^2}{\lambda_n^2 + m_1^2} + O(m_1). \quad (4.6)$$

Since in this sum we only keep terms for which $l_n \leq l$, this may be expressed more simply as

$$m_1 \tilde{\Gamma}(p) \geq \pi \rho_l(0) (1 - c_2 l^2 p^2) + O(m_1). \quad (4.7)$$

Here $\rho_l(\lambda)$ is the density of exponentially localized eigenstates (according to our definition (4.1)) with eigenvalue λ and localization range less than or equal to l .

This result is of key importance. It establishes that if there is a non-zero density of near-zero modes which are exponentially localized within a certain range l , the pion two-point function diverges as $m_1 \rightarrow 0$ in any finite volume, for all momenta p below (roughly) the inverse localization range. As we will argue in Sect 4.2 below, the analysis of Ref. [23] allows us to establish the same result in the infinite-volume limit, provided the mobility edge does not vanish (and m_0 is in the super-critical region). This provides an alternative mechanism for saturating the Ward identity, Eq. (2.11), in the presence of a non-vanishing pion condensate $\langle \pi_3 \rangle$. It also shows that the quenched theory in infinite volume is not well defined for $m_1 = 0$, at least as long as the mobility edge does not vanish.

A comment is in order on the range of momenta for which our result is valid, because of the fact that in a finite volume the momenta are discrete, and thus cannot be chosen arbitrarily small. First, we observe that for a localized near-zero mode, the scale of the typical localization range l is set by the inverse mobility edge, λ_c^{-1} .

(This will be explained in more detail in the following subsection.) As long as we are not close to the Aoki phase, this is of order one in lattice units. With the smallest lattice momenta being of order $1/L$, we may choose the volume large enough that $c_2(l/L)^2 \ll 1$, so that non-zero momenta indeed exist for which the right-hand side of Eq. (4.7) is positive.

4.2 Spontaneous symmetry breaking without Goldstone excitations

We are now at a point where we wish to collect all the available results, and use them to construct a conjecture for the quenched phase diagram. The goal is to combine the numerical [20, 21] as well as the analytical [23] evidence that basically everywhere in the super-critical region the density of near-zero modes does not vanish (already in finite volume) with the inequality for the pion two-point function, Eq. (4.7). In a sense, we will be proposing the simplest possible picture of what determines the phase diagram, while requiring consistency with the Ward identity (2.11). While we already summarized our conjecture for the phase diagram in the introduction, we present a more detailed discussion in this subsection.

A key element is the observation made by BNN in Ref. [23], that in the super-critical region there will be a density of near-zero modes. We will therefore start with elaborating on this observation. As already alluded to in the introduction, it will lead us to borrow the concept of the “mobility edge” from condensed-matter physics as the crucial ingredient in determining the quenched phase diagram.

Following BNN, we begin with an infinite-volume configuration containing a single dislocation. We pick a lattice gauge field which is equal to the classical vacuum ($U_{x\mu} = I$) everywhere, except for the links of an n^4 hypercube containing the origin. These links can take any value. The square of the Wilson–Dirac operator can be written as

$$H^2(m_0) = H_0^2(m_0) + V, \quad (4.8)$$

where $H_0(m_0)$ is the free operator. The potential V is supported on an $(n+2)^4$ hypercube. The “hamiltonian” $H^2(m_0)$ is a discretized, semi-positive Schrödinger operator with a finite-range potential, with a continuum threshold at $(\lambda_{min}^0)^2$ (*cf.* Sect. 2). All eigenstates with $(\lambda_{min}^0)^2 < E < (\lambda_{max}^0)^2$ are scattering states, while those with $0 \leq E < (\lambda_{min}^0)^2$, if they exist, are bound states of $H^2(m_0)$ with “binding energy”

$$-E_b \equiv E - (\lambda_{min}^0)^2 < 0. \quad (4.9)$$

Of course, bound-state wave functions decrease exponentially away from the hypercube, with a decay rate determined by E_b^{-1} . In particular, a zero mode has $E = 0$, and thus a binding energy $E_b = (\lambda_{min}^0)^2$.

For single-dislocation configurations, BNN proved that the problem of finding a zero mode in large (or infinite) volume can be reduced to a corresponding eigenvalue problem on the small hypercube. Solving the latter problem numerically BNN then found that, for $-1 > am_0 > -7$ (roughly), the links of a hypercube as small as 2^4 can always be chosen such that $H(m_0)$ has an eigenvalue equal (or numerically extremely

close) to zero. This means that, for that range of m_0 , zero modes exist for any volume down to 2^4 . Moreover, these zero modes are exponentially localized (as long as m_0 is not equal to one of its critical values). We note that BNN configurations are examples of exceptional configurations.⁷

It is not implausible that, by allowing for larger dislocations, exponentially-localized zero modes would be found throughout virtually the entire super-critical interval $0 > am_0 > -8$. One does expect that, to get a zero eigenmode closer to a boundary point of the super-critical interval, the gauge field would have to differ from the classical vacuum over bigger hypercubes. In this paper, we will assume that this is the case, *i.e.* that for any am_0 strictly inside the interval $(-8, 0)$, BNN-like zero modes will be found.

Before continuing, let us comment on the nature of typical zero modes, and the configurations supporting them. An exact zero mode of $H^2(m_0)$ is also a zero mode of $H(m_0)$. As one varies the lattice gauge field, a zero eigenvalue generically corresponds to a zero-level crossing, because with Wilson fermions there is no chiral symmetry that might protect a zero eigenvalue from moving away from zero. In other words, if $\mathcal{U}(\tau) \equiv \{U_{x\mu}(\tau)\}$ is a family of gauge-field configurations that depend smoothly on τ , and if there is an eigenvalue λ_n such that $\lambda_n(\mathcal{U}(0)) = 0$ then, typically, $\lambda_n(\mathcal{U}(\tau))$ changes sign at $\tau = 0$. This is true for (almost) all exceptional configurations which support exact zero modes. It implies that any finite-volume configuration supporting an (exponentially localized) exact zero mode has some open neighborhood, in the gauge-field space, with a spectrum of near-zero modes. Also, in a finite volume, the subspace of configurations that support an exact zero mode has codimension one.

Our next step is to consider configurations containing a very small density of BNN-like dislocations. The dislocations are small, surrounded by the classical vacuum, and (still, on average) far apart. This is a “controlled” form of *disorder*. The origin of disorder is two-fold: the positions of the dislocations are chosen at random (one can speak about a dilute gas of dislocations); also the links that define each dislocation are chosen at random. A unique limiting value $\lim_{|x| \rightarrow \infty} V(x)$ of the potential in Eq. (4.8) no longer exists, because dislocations may be found arbitrarily far from the origin.

As long as the gas of dislocations is dilute, we can still identify all dislocations separately from the surrounding vacuum, simply by inspection. So, let us focus on one dislocation, and assume that in isolation (*i.e.* with no other dislocations anywhere), it has an exact zero mode. Since the other dislocations are far apart, they will have a negligible effect on this zero mode. This is easily seen by invoking a variational argument. Using the eigenfunction of the zero mode of the isolated dislocation as a trial wave function, the expectation value of $H^2(m_0)$ on this trial state will receive contributions only from the other distant dislocations. If the mean distance between dislocations is R , the expectation value of $H^2(m_0)$ will be of order $e^{-2\gamma}$ where $\gamma \sim \lambda_{min}^0 R$. Therefore $H^2(m_0)$ must have an eigenstate with an exponentially small eigenvalue $E \sim e^{-2\gamma}$ which closely resembles the original zero mode. We may now

⁷Even though we expect BNN configurations to amount to only a tiny subset of all exceptional configurations.

vary the gauge field at the dislocation such that the eigenvalue under consideration varies as well. As long as R is large enough (compared to $1/\lambda_{min}^0$), $e^{-2\gamma}$ is small enough that this gauge-field variation will vary the eigenvalue over an interval that includes zero.

The situation changes qualitatively if the density of dislocations is large, and also will be different for configurations generated in a typical Monte-Carlo simulation. In order to describe this situation, it will be useful to introduce the *mobility edge hypothesis* [27]. The mobility edge is well-defined only in infinite volume, and we will thus assume the volume to be infinite for the following discussion. The hypothesis states that, when disorder is introduced in an ordered system, the conduction-band structure of the ordered system is replaced by a number of alternating energy intervals, each containing either (exponentially) localized or extended eigenstates. In particular, no energy exists for which there are both localized and extended eigenstates.⁸ The energy separating an interval with localized modes from one with extended modes is referred to as a mobility edge.

Intuitively, a mobility edge arises as follows. Let us first return to a situation with “controlled” disorder consisting of a dilute gas of BNN dislocations. As already mentioned, for a very small density of dislocations, all bound states with $E_b = O(1/a^2)$ (see Eq. (4.9)) will be exponentially localized near a single dislocation. As the density of dislocations is increased there is an increased probability that an “electron,” situated initially in a bound state of a given dislocation, will tunnel into a near-by dislocation. When the probability to tunnel a certain distance times the average number of available dislocations within this distance has become $O(1)$ for some given E , the electron will be able to travel infinitely far by tunneling from dislocation to dislocation, regardless of the details of the dislocation that produced the original bound state. In other words, the eigenstate with eigenvalue E becomes extended.

For a single dislocation, any eigenstate with $E < (\lambda_{min}^0)^2$ decays exponentially. Increasing E means a slower decay rate and, hence, an increased tunneling probability. This means that eigenstates with higher E become extended first when the density of dislocations is increased. If λ_c^2 is the mobility edge, the range $0 \leq E \leq \lambda_c^2$ will consist of exponentially localized eigenstates, while the range $E \geq \lambda_c^2$ consists of extended ones. For a very small density of dislocations the mobility edge will be close to $(\lambda_{min}^0)^2$, while for larger densities it will move further away from this value. If, for instance, we allow only dislocations generating an attractive potential in Eq. (4.8), the mobility edge will clearly be lower than $(\lambda_{min}^0)^2$.

We note that there may exist more than one mobility edge at a given location in the phase diagram. For instance, if the hamiltonian is bounded from above, one expects another mobility edge to occur, *above* which other localized eigenstates exist. In our case, we expect a second mobility edge like this, because the eigenvalue spectrum of the free hamiltonian, $H_0^2(m_0)$ in Eq. (2.2), also has a maximum eigenvalue $(\lambda_{max}^0)^2$. In this paper, we will be concerned with the lowest-lying mobility edge, and in particular, the question of whether it vanishes or not.

Now consider the hypothetical situation that, for a certain gauge-field configura-

⁸We are not aware of any proof of this—widely used—assertion.

tion, both extended and localized eigenstates of the hamiltonian $H^2(m_0)$ occur at the same energy E . If we then calculate the eigenstates on a typical small fluctuation of this gauge field, the extended and localized states will mix, and all new eigenstates will be extended. The only possible exception is when all eigenstates of the original gauge field were localized. A “typical” configuration thus has either only extended or only localized eigenstates at a given E . Since typical configurations (in this sense) determine the properties of an ensemble, it follows that the value of a mobility edge separating localized and extended eigenstates is associated with an equilibrium ensemble, and thus with a point (m_0, g_0) in the phase diagram. Another way of arriving at the same conclusion is to note that in the thermodynamic limit, one equilibrium configuration suffices to determine the equilibrium properties of the theory, and thus is typical. For our purposes, it will be useful to characterize each point (am_0, g_0) in the phase diagram by the value of the lowest mobility edge of $H^2(m_0)$. (In the rest of this paper, we will refer to this mobility edge as “the” mobility edge.) The mobility-edge hypothesis will be at the heart of our conjecture for the phase diagram of quenched QCD.

Before we get to this conjecture, let us briefly comment on the average localization range as a function of E . For energies at which only localized states exist, one expects to be able to define an average localization range $\bar{l} = \bar{l}(E)$. This average localization range should then grow if the energy E approaches the mobility edge, and diverge at and beyond the edge, where only extended eigenstates exist.

Based on BNN’s results we expect that anywhere inside the super-critical region there will be a non-zero density of near-zero modes. If the mobility edge is zero this expectation is fulfilled by assumption. If the mobility edge is larger than zero, then, for any $0 > am_0 > -8$ and $g_0 > 0$, there is a finite probability per unit volume that any given Monte-Carlo configuration will contain a ball with (a large) radius R , inside which the configuration will resemble the classical vacuum, apart from a single BNN dislocation well inside that ball. Using the same variational argument as in the dilute-gas case, the exact BNN zero mode associated with the dislocation implies the existence of an eigenstate with eigenvalue $e^{-2\gamma} \ll \lambda_c^2$, well below the mobility edge. This eigenstate decays exponentially both inside and outside of the classical-vacuum ball. By invoking small deformations of this configuration, the existence of a density of exponentially localized near-zero modes follows.⁹

We now formulate our main conjecture about the phase diagram of quenched QCD with two Wilson fermions. Near the line $g_0 = 0$, we expect the mobility edge to be very close to $(\lambda_{min}^0)^2$. In particular, with $(\lambda_{min}^0)^2$, it will vanish at the critical “end” points $g_0 = 0, am_0 = 0, -2, -4, -6, -8$. As g_0 is increased and the typical gauge-field configuration in an equilibrium ensemble becomes less smooth, the mobility edge will move away from $(\lambda_{min}^0)^2$, and, in parts of the phase diagram, it may vanish. Since

⁹A zero-level crossing in the spectrum of $H(m_0)$ changes the index of the overlap operator. This index was advocated as a definition of the topological charge on the lattice [4, 5]. However, standard arguments imply that the topological charge density scales like $1/\sqrt{V}$ in large volume, and, thus, vanishes for $V \rightarrow \infty$ (see *e.g.* Ref. [31]). Therefore, topological considerations do not explain a non-zero density of near-zero modes in the infinite volume limit. This situation reflects the inherent ambiguity in trying to identify small dislocations as instantons or as anti-instantons.

it vanishes at the critical end points on the $g_0 = 0$ axis, it is reasonable to expect that the mobility edge will also vanish in the vicinity of those points for $g_0 > 0$, thus opening up the finger-like structure of region B in Fig. 1. In a region where the mobility edge vanishes, the density of near-zero modes will be due to extended near-zero modes, and one expects long-range behavior, in particular Goldstone excitations. We thus conjecture that, in quenched QCD, the Aoki phase—which is defined as the phase in which Goldstone excitations exist—coincides with the region of the phase diagram where the mobility edge vanishes. The near-zero mode density, and thus the value of $\langle \pi_3 \rangle$, is due to extended eigenstates. Outside the Aoki phase (but inside the super-critical region), the mobility edge is larger than zero, and the density is due to exponentially localized near-zero modes. Because of this non-vanishing density, the mechanism derived in the previous subsection will kick in, and the pion two-point function will diverge for $m_1 \rightarrow 0$ for small-enough momenta.

Extended states should not contribute to the $1/m_1$ divergence in the infinite-volume limit. The number of extended states grows like the volume V , whereas the contribution to Eq. (3.3) of each extended state drops like $1/V^2$. This yields a contribution of order $1/V$, which vanishes for $V \rightarrow \infty$. Therefore, we expect no $1/m_1$ divergence of the pion two-point function inside the Aoki phase; the $1/m_1$ divergence characterizes region C (and the super-critical part of region A) of the phase diagram. It follows that, while $\langle \pi_3 \rangle$ is not a useful order parameter for detecting the Aoki phase, the residue of a $1/m_1$ divergence in $\tilde{\Gamma}(p)$ (for small enough momentum) is a useful order parameter in this sense. There is even a *local* order parameter associated with this divergence:

$$\xi(x) \equiv \lim_{m_1 \rightarrow 0} m_1 \Gamma(x, x) = \lim_{m_1 \rightarrow 0} m_1 \langle \pi_+(x) \pi_-(x) \rangle . \quad (4.10)$$

This follows from $\xi(x) = (1/V) \sum_p \tilde{\Gamma}(p)$, the bound (4.7), and the positivity of $\tilde{\Gamma}(p)$ for all p .

We believe that essentially the same conjecture holds for *unquenched* QCD. The only difference is that in the unquenched case, the spectral density $\rho(0)$ (and thus the order parameter) vanishes outside the Aoki phase, because of the suppression of the localized near-zero modes by the fermion determinant (*cf.* Sect. 5). Therefore, also the $1/m_1$ divergence in the pion two-point function will not occur in the unquenched case. These phenomena are quenched artifacts, but the existence and role of the mobility edge are not. To summarize, the qualitative features of the phase diagram in Fig. 1 are valid in both quenched and unquenched QCD. The mobility edge λ_c is zero in region B, and non-zero outside of this region, where exponentially localized modes with $\lambda^2 < \lambda_c^2$ exist. In regions C and in the super-critical part of regions A the spectrum of localized modes extends down to zero, with the only difference that $\rho(\lambda) > 0$ for $\lambda^2 \geq 0$ in the quenched theory, and for $\lambda^2 > 0$ in the unquenched theory.

Clearly, our picture of the phase diagram proposed here is a conjecture, and we have no proof that it is correct. We emphasize that it appears to be the simplest possible way one can understand the phase diagram, given the available analytical and numerical evidence. We will end this section with a more quantitative, but still heuristic argument as to why Goldstone excitations *only* occur in the phase with

vanishing mobility edge.

We will assume that outside the Aoki phase, the near-zero-mode density $\rho(0)$ is entirely due to localized zero modes captured by our bound, Eq. (4.1). Moreover, we will assume that, for practical purposes, a maximum localization length l_{max} exists for the near-zero modes. Hence¹⁰ $\rho_{l_{max}}(0) = \rho(0)$, and, using both the lower and upper bounds in Eq. (4.2),

$$\pi\rho(0)(1 - c_2 l_{max}^2 p^2) \leq \lim_{m_1 \rightarrow 0} m_1 \tilde{\Gamma}(p) \leq \pi\rho(0). \quad (4.11)$$

Writing $\tilde{\Gamma}_\mu(p) = ip_\mu \Sigma(p^2)$, it then follows from the Ward identity, Eq. (2.11) that

$$\Sigma(0) = 2\pi\rho(0) O(l_{max}^2), \quad (4.12)$$

leading to the conclusion that $\tilde{\Gamma}_\mu(p)$ does not have a massless pole.

The most drastic assumption we make here is that there is a finite l_{max} . This is rather unlikely, even if it is reasonable to expect that the probability to find a near-zero mode with a very large localization range at some point well outside the Aoki phase is very small. In order to argue that also in this case no Goldstone poles occur outside the Aoki phase, clearly one needs a better estimate of $|\mathcal{H}_n(p)|$ than that provided by the bounds given in Eq. (4.2). While it is a very hard problem to come up with better estimate, we will use an *ansatz* for a better estimate to show how an improved argument might work. Let us assume that $|\mathcal{H}_n(p)|$ can be estimated by

$$|\mathcal{H}_n(p)| \sim \frac{1}{1 + p^2 l_n^2}, \quad pa \ll 1. \quad (4.13)$$

This is not unreasonable for momenta $p \ll 1/a$. For very small momenta, one expects only the long-distance features of the near-zero modes, *i.e.* the exponential tail in Eq. (4.1), to determine the Fourier transform of $|\Psi_n(x)|^2$, and thus $|\mathcal{H}_n(p)|$ would have to look something like this. The precise form is not important; the crucial properties of this *ansatz* are that it is bounded for arbitrary l_n , and that it is consistent with the fact that $|\mathcal{H}_n(0)| = 1$, as follows from the fact that $\Psi_n(x)$ is normalized to one.

If $\rho(0)$ is completely due to localized near-zero modes, we may write $\rho(0) = \int_0^\infty dl \rho'_l(0)$ with $\rho'_l(\lambda) = d\rho_l(\lambda)/dl$, and Eq. (3.4) as

$$\begin{aligned} \lim_{m_1 \rightarrow 0} 2m_1 \tilde{\Gamma}(p) &\sim \frac{2\pi}{V} \int_0^\infty dl \int \mathcal{DUB}(\mathcal{U}) \sum_n \delta(\lambda_n) \delta(l - l_n) \frac{1}{(1 + p^2 l^2)^2} \\ &= 2\pi \int_0^\infty dl \rho'_l(0) \frac{1}{(1 + p^2 l^2)^2}. \end{aligned} \quad (4.14)$$

Combining this with Eqs. (2.11) and (2.15) we obtain the estimate

$$\Sigma(p^2) \sim 2\pi \int_0^\infty dl \rho'_l(0) \frac{2l^2 + p^2 l^4}{(1 + p^2 l^2)^2}, \quad (4.15)$$

showing again that $\tilde{\Gamma}_\mu(p)$ has no massless pole. We note that the integral over l should be convergent because $d\rho_l(0)/dl$ should be strongly suppressed for large l .

¹⁰Recall that $\rho_l(\lambda)$ is the density of localized eigenstates with localization range less than l .

This completes our discussion of the quenched phase diagram. In the remainder of this paper, we will expand on the differences between the quenched and unquenched cases, and explore the consequences for domain-wall and overlap fermions.

5. Unquenched QCD

In this section we only review well-known facts about unquenched QCD. The only reason we include this brief review is to point out that none of the surprising results we obtained in the previous section for quenched QCD are in conflict with the standard lore in the unquenched theory.

5.1 Vanishing of the condensate in finite volume and absence of localized near-zero modes

We start with a review of the proof that the finite-volume condensate is zero in unquenched QCD. Summing the Ward identity (2.9) over space-time, the total-derivative term drops out, and we obtain

$$2m_1 a^4 \sum_x \langle \pi_+(x) \pi_-(y) \rangle = \langle \pi_3 \rangle . \quad (5.1)$$

In a finite volume, the correlation function of the product of any (finite) number of fermion (and link) operators is bounded. The left-hand side of Eq. (5.1) is therefore the product of m_1 with a bounded function, hence it vanishes for $m_1 \rightarrow 0$. It follows that the condensate vanishes. This is the familiar result that there is no spontaneous symmetry breaking in a finite volume.

In order to prove boundedness, consider first the unnormalized expectation value of any observable made of a product of (link and) fermion fields. Because of the Berezin integration rules for Grassmann variables, the Wick contraction of the fermion fields leads to a function which is analytic in the parameters of the fermion action m_0 and m_1 . Integrating also over the (compact) link variables of the gauge field leaves an unnormalized expectation value which again is an analytic function of these variables, including for $m_1 = 0$. Similarly the partition function Z is strictly positive for a two-flavor theory with Wilson fermions (for $g_0 > 0$), and again Z^{-1} is bounded for a bounded range of values of m_0 and m_1 which includes $m_1 = 0$. Hence normalized expectation values are bounded as well. In contrast, in quenched QCD the fermion determinant is missing, and a fermionic observable may diverge if the Wilson–Dirac operator has near-zero modes. This is what happens in the case of the pion two-point function.

It follows, through the Banks–Casher relation, that $\rho(0) = 0$. Since $0 \leq \rho_l(0) \leq \rho(0)$, one has $\rho_l(0) = 0$ for any finite volume. While of course the infinite volume is subtle (and does not commute with the limit $m_1 \rightarrow 0$), we believe that for any finite l , $\rho_l(0)$ will remain zero in the infinite-volume limit, because $\rho_l(0)$ reflects short-distance physics. Also, if the inequality (4.7) remains valid in the infinite-volume limit on the

one hand, and unquenched QCD does not have a $1/m_1$ divergence on the other hand, clearly $\rho_l(0)$ must remain zero in that limit. The fact that a $1/m_1$ divergence indeed cannot occur in unquenched QCD is explained in the next subsection.

5.2 The Goldstone theorem

Here we re-derive the Goldstone theorem in the euclidean path-integral context in infinite volume (for a review see Ref. [32]). For simplicity, we do this in the continuum; nothing relevant changes on the lattice. As in the previous subsection our aim is to show that the (Fourier-transformed) pion two-point function $\tilde{\Gamma}(p)$ is bounded in a neighborhood of $m_1 = 0$ but now for $p \neq 0$ (and without assuming that the condensate necessarily vanishes). We may then again conclude that, for $p \neq 0$, $2m_1\tilde{\Gamma}(p) \rightarrow 0$ for $m_1 \rightarrow 0$. Taking this limit, the Ward identity (2.11) yields (dropping terms of order ap)

$$ip_\mu \tilde{\Gamma}_\mu(p) = \langle \pi_3 \rangle, \quad p \neq 0. \quad (5.2)$$

If the condensate is non-zero (*i.e.* if SSB takes place), this implies the existence of a massless Goldstone pole in $\tilde{\Gamma}_\mu(p)$.

To prove the boundedness of $\tilde{\Gamma}(p)$ for $p \neq 0$, we invoke the Källén-Lehmann representation. A one-particle contribution to $\tilde{\Gamma}(p)$ must be of the form $|F|^2/(p^2+M^2)$ where M is the particle's mass and F is a form factor which is non-zero on shell ($p^2 = -M^2$). For any non-zero euclidean momentum,

$$\frac{m_1}{p^2 + M^2} \leq \frac{m_1}{p^2}, \quad p \neq 0. \quad (5.3)$$

The right-hand side of inequality (5.3) provides a bound for the contribution of any one-particle excitation to $2m_1\tilde{\Gamma}(p)$, implying that it vanishes in the limit $m_1 \rightarrow 0$, for $p \neq 0$. This is true also if the particle's mass vanishes in the same limit (as in the case of a Goldstone boson). The contributions of multi-particle states will be less infra-red singular, and should also vanish. In summary, in unquenched QCD, $2m_1\tilde{\Gamma}(p)$ vanishes in the thermodynamical limit, for $p \neq 0$.

The quenched theory is not unitary, and the Källén-Lehmann representation for the pion two-point function invoked above is not valid. Apparently, nothing stops the pion two-point function from developing a $1/m_1$ divergence.

6. Implications for domain-wall and overlap fermions

The most common constructions of lattice Dirac operators with domain-wall or overlap fermions employ the Wilson-Dirac operator discussed in this paper (or improved versions thereof) as a kernel.

Domain-wall fermions are five-dimensional Wilson fermions, in which only hopping terms in the four physical directions couple to four-dimensional link variables, which themselves are independent of the fifth coordinate [2, 3]. In the most common

version, the fifth dimension is restricted to a finite interval of length $a_5 N_s$, where a_5 and N_s are respectively the lattice spacing and number of sites in the fifth direction. Free boundary conditions are employed on either side (in the limit of a vanishing physical quark mass). In the limit $N_s \rightarrow \infty$, massless four-dimensional fermions appear which are bound to the two boundaries. If the left-handed component of this massless fermion is bound to one boundary, the right-handed component is bound to the other one. For $g_0 \rightarrow 0$, precisely one such massless fermion appears (per five-dimensional fermion field) if the domain-wall height $M = -m_0$ is chosen such that $0 < a'M < 2$ where $a' = \max\{a, a_5\}$ [33]. This means that m_0 has to be super-critical.

The overlap-Dirac operator is defined as [5]

$$aD_{ov} = 1 - \gamma_5 \hat{\gamma}_5, \quad \hat{\gamma}_5 \equiv \frac{H(m_0)}{|H(m_0)|}, \quad (6.1)$$

with $H(m_0)$ the hermitian Wilson-Dirac operator. Notice that $\hat{\gamma}_5^2 = 1$. For this operator to describe one massless flavor in the continuum limit, one needs to choose $0 > am_0 > -2$.

Because of the fact that $H(m_0)$ plays a crucial role in the construction of domain-wall/overlap fermions, it is natural to expect that the phase diagram of QCD with Wilson fermions has important implications for properties of domain-wall/overlap fermions. The most important dynamical issue is whether the mobility edge is (close to) zero, or not. In this section, we will argue that in order to retain locality in lattice QCD with overlap fermions, the parameters of the lattice theory must be chosen well outside the Aoki phase. For domain-wall fermions the situation is equivalent: only well outside the Aoki phase will chiral symmetry be restored exponentially fast with increasing N_s . In addition, only in that case will the four-dimensional effective theory (which is described by a generalized overlap operator, the details of which depend on a_5) be local in the limit $N_s \rightarrow \infty$.

In the quenched case, we may say that lattice QCD with domain-wall/overlap fermions is inside or outside the Aoki phase if the “underlying” theory with the Wilson-Dirac operator $H(m_0)$ is. One may think of the phase diagram as that of a theory with N_f quenched domain-wall/overlap flavors *and* two quenched Wilson flavors. Of course, this changes nothing in the correlation functions of the domain-wall/overlap quarks. What it means is that, also in the domain-wall/overlap case, we define the quenched Aoki phase by the existence of a Goldstone pole in the appropriate correlation function constructed from the inverse of the Wilson-Dirac operator $H(m_0)$ (*cf.* Eq. (2.8)), using the same value of m_0 as in the kernel of the domain-wall/overlap operator, and the same Boltzmann weight. According to our conjecture, this corresponds to the region in parameter space in which the mobility edge of $H(m_0)$ vanishes.

In the unquenched case, the only thing that changes is the Boltzmann weight used to generate the ensemble of gauge-field configurations on which the domain-wall or overlap operator is computed.¹¹ For any given ensemble, the mobility edge of

¹¹Note that the fermion determinant used for generating the gauge-field configurations may correspond to any type of lattice fermion. If the sea quarks and the valence quarks are not coming from the same fermion action, one is dealing with a partially quenched theory [34].

the Wilson–Dirac kernel $H(m_0)$ should have a well-defined value. We may thus still define the Aoki phase as that region in parameter space in which the mobility edge of $H(m_0)$ vanishes. Conversely, if the mobility edge does not vanish, we will say that we are outside the Aoki phase for the unquenched theory.

Let us start with locality of the overlap operator. The overlap operator $D_{ov}(x, y)$ cannot have a finite range [35], and thus is not strictly local for a finite lattice spacing. However, Hernández, Jansen and Lüscher proved that the overlap is local in the sense that $|D_{ov}(x, y)|$ decays exponentially with the distance $|x - y|$, provided the gauge field obeys an admissibility condition [36]. The effect of this condition is to secure an $O(1/a)$ gap in the spectrum of $H(m_0)$ (except very close to the critical values of m_0). They furthermore generalized this result to the case that $H(m_0)$ has an isolated zero mode inside an otherwise empty spectral gap by showing that such a mode is necessarily exponentially localized. The rate of the exponential decay of the overlap operator in these cases is of order one in lattice units.

The problem is that, for realistic simulations, it is impractical to impose an admissibility condition on the gauge fields. If instead one uses one of the commonly used local gauge actions to generate an equilibrium ensemble, $H(m_0)$ will have (localized) eigenmodes with very small eigenvalues, and these eigenvalues will not be isolated in the sense of Ref. [36]. In fact, since the number of localized modes grows in proportion to the volume, in the infinite-volume limit the eigenvalues of the localized modes will form a dense set, and no eigenvalue will be isolated. This is most clear in the quenched case, where $\rho(0)$ is always non-zero in the super-critical region.

At this point we invoke our physical picture of the phase diagram. For any $g_0 > 0$, the band edge λ_{min}^0 (of the free hamiltonian $H_0(m_0)$) gets replaced by the mobility edge λ_c . We hypothesize that, as long as $\lambda_c > 0$, the conclusion of Ref. [36] still holds: if all near-zero modes are exponentially localized with a finite average localization length \bar{l} , then $\hat{\gamma}_5$ (and thus D_{ov}) decays exponentially. As we argue below, the decay rate is in principle governed by the smaller of λ_c and $1/\bar{l}$. We expect this situation to apply inside phase C in Fig. 1, well outside the Aoki phase. In fact, if we assume, like at the end of Sect. 4.2, that the near-zero modes have a finite maximal localization length l_{max} outside the Aoki phase, our hypothesis is simple to prove.

First, however, let us consider the corresponding situation with domain-wall fermions. The relevant Ward identity [3] for the study of the finite- N_s chiral symmetry breaking with domain-wall fermions is, for $x \neq y$,

$$\partial_\mu^* \langle A_\mu^a(x) J_5^b(y) \rangle = 2m_q \langle J_5^a(x) J_5^b(y) \rangle + 2 \langle J_{5q}^a(x) J_5^b(y) \rangle. \quad (6.2)$$

Here A_μ^a is the domain-wall partially-conserved axial current and J_5^b is the corresponding pseudo-scalar quark density (a, b label flavor generators); m_q is the quark mass. J_{5q}^a is a pseudo-scalar density located midway between the boundaries of the five-dimensional bulk. The term containing this density represents the chiral symmetry breaking at finite N_s other than the expected breaking coming from an explicit quark mass. For chiral symmetry to be restored, it should vanish in the $N_s \rightarrow \infty$ limit for non-singlet axial currents. (In the case of the axial U(1) current this term gives rise to the anomaly in the continuum limit.)

In order to study chiral symmetry restoration, it is useful to consider the transfer matrix $T(M, a_5)$ which hops in the fifth direction, from one four-dimensional “time” slice to the next [3, 4]. For every eigenmode Ψ_n of $T(M, a_5)$ with (positive¹²) eigenvalue ω_n , we let $q_n = \min\{\omega_n, \omega_n^{-1}\}$. Hence, $0 < q_n \leq 1$. In the *second-quantized* transfer matrix, the replacement of ω_n by q_n reflects normal ordering. For the free theory the transfer matrix has a gap: $q_n \leq q_0$ for all eigenmodes, where $q_0 < 1$. We refer to q_0 as the band edge of the free transfer matrix. (As an example, in the special case where $aM = a_5/a = 1$, one has $q_0 = 1/2$.) In the interacting theory, we define the mobility edge of the transfer matrix as $q_c = \max\{q_n\}$, where the maximum is taken over the extended modes only. Below, we will also speak of the “hamiltonian” $H(-M, a_5) \equiv -\log(T(M, a_5))/a_5$. This hamiltonian has a band edge $-\log(q_0)/a_5$ in the free theory, and a mobility edge $\lambda'_c = -\log(q_c)/a_5$ in the interacting theory. (In the limit $a_5 \rightarrow 0$ one recovers the familiar Wilson–Dirac operator: $H(-M, 0) = H(-M)$, and λ'_c reduces to λ_c .)

Since the transfer matrix has a gap in the free theory, the four-dimensional massless fermions at the boundaries are exponentially bound to their respective boundaries. If we take $N_s \rightarrow \infty$ at fixed M and a_5 , we find an exponentially decreasing overlap between the (fifth-coordinate) wave functions of the light-quark modes tied to the boundaries and the “midway” pseudo-scalar density J_{5q}^a . Hence chiral symmetry gets restored exponentially in N_s . With gauge fields obeying an admissibility condition, the situation remains the same, because the transfer matrix still has a gap. Also, with commonly used local gauge actions, a similar behavior has been demonstrated in weak-coupling perturbation theory [37, 38].

Non-perturbatively, one can prove that, for any a_5 , a zero mode of the Wilson kernel is also an eigenstate with eigenvalue one of the transfer matrix: $T(M, a_5)\Psi_n = \Psi_n$ if and only if $H(-M)\Psi_n = 0$ [3, 4]. This implies that $H(-M)$ and $H(-M, a_5)$ have a similar spectrum of near-zero modes. A near-zero mode of $H(-M, a_5)$ causes long-range correlations in the s direction. This means that in realistic simulations with commonly used gauge actions, configurations will occur for which the last term in Eq. (6.2) may be large, thus “threatening” the chiral symmetry of domain-wall fermions even in the large- N_s limit. This danger is again brought out most clearly in the quenched case, where a non-zero density of near-zero modes always occurs for the above specified range of M .

However, we hypothesize that, in analogy with the overlap case, there is a fundamental difference between the effect of exponentially localized near-zero modes and that of extended ones. If all near-zero modes of $H(-M, a_5)$ are exponentially localized with an average localization length \bar{l} , we expect their contribution to the symmetry-breaking term in Eq. (6.2) to decay exponentially as a function of the *four-dimensional* separation $|x - y|$. If the scale of \bar{l} is set by the (four-dimensional) lattice spacing, this decay will resemble a contribution from excitations with mass of the order of the cutoff. When the lattice spacing is small enough, even at finite N_s this contribution

¹²For a certain range of M and a_5 the transfer matrix may have real but negative eigenvalues; in this case the entire analysis can be carried out in terms of the transfer-matrix squared (provided N_s is a multiple of four).

will vanish for large $|x - y|$ relative to the other two terms in Eq. (6.2), whose long-distance behavior is determined by a *physical* mass. All other contributions to the symmetry-breaking term will not be suppressed with the four-dimensional separation, but they will vanish exponentially with N_s .

Similar conclusions apply to the locality of the effective four-dimensional lattice Dirac operator in the $N_s \rightarrow \infty$ limit [39]. This is a generalized overlap operator constructed by making the replacement $H(-M) \rightarrow H(-M, a_5)$ in Eq. (6.1). Because of the similar zero-mode structure of $H(-M)$ and $H(-M, a_5)$, we expect the effective Dirac operator to be local (in the exponential sense) well outside the Aoki phase, as in the case of the overlap discussed above.

For both domain-wall and overlap fermions, these arguments break down if the near-zero modes are extended, or even, if $1/\bar{l}$ becomes of the same order as the numerical values of the physical masses in a particular simulation. This latter situation is expected close to the Aoki phase, because \bar{l} will increase going towards the phase transition, and become infinite at the phase transition. The domain-wall formalism gives a clear indication on what may go wrong inside the Aoki phase. When the mobility edge of the Wilson kernel $H(-M)$ (or, more generally, of $H(-M, a_5)$) is zero, there are massless excitations everywhere *inside* the five-dimensional bulk. Normally, the contribution of the *massive* bulk modes is canceled by Pauli-Villars (pseudo-fermion) fields. But there is absolutely no guarantee that that cancellation will persist when the bulk fermion and pseudo-fermion modes are massless: this situation corresponds to a different phase of the theory. The limit $N_s \rightarrow \infty$ now involves infinitely many unphysical, light four-dimensional fields (arising from both the five-dimensional domain-wall and the pseudo-fermion fields), and we have every reason to worry that the limiting theory is not what we want it to be. This is true for any a_5 , and thus also in the overlap limit $a_5 \rightarrow 0$.

We now present a more detailed argument as to why the overlap operator should be local well outside the Aoki phase. We will assume, as we did at the end of Sect. 4.2, that at a given point well outside the Aoki phase there exists a finite maximum localization length for the near-zero modes of $H(m_0)$. In fact, to avoid technical complications, it is convenient to make a slightly stronger assumption, namely, that if $\lambda_c > 0$ is the mobility edge, then all eigenstates with $-\lambda_c/2 < \lambda < \lambda_c/2$ have a bounded localization length $l \leq l_{max} < \infty$. As before, this assumption is not unreasonable because the average localization length diverges only for $|\lambda| \nearrow \lambda_c$, and the probability for arbitrarily large localization lengths is expected to vanish rapidly (and uniformly) for any $|\lambda| < \lambda_c/2$. By simply replacing $H(m_0)$ by $H(-M, a_5)$, the below argument may also be applied to the $N_s \rightarrow \infty$ limit of domain-wall fermions.¹³

We begin by noting that the overlap operator D_{ov} is local if $\hat{\gamma}_5$ is local. We split

$$\hat{\gamma}_5 = \hat{\gamma}_5^< + \hat{\gamma}_5^>, \quad (6.3)$$

where $\hat{\gamma}_5^<$ is the projection of $\hat{\gamma}_5$ onto the subspace spanned by eigenstates with eigenvalue $|\lambda| < \lambda_c/2$. On the basis of eigenmodes of $H(m_0)$, $\hat{\gamma}_5^<$ can be represented

¹³For small a_5 one can also use Borici's kernel [40] $\gamma_5 D(-M)(2 - a_5 D(-M))^{-1}$ that gives rise to the same generalized overlap operator as $H(-M, a_5)$.

as

$$\hat{\gamma}_5^<(x, y) = a^4 \sum_{|\lambda_n| < \lambda_c/2} \Psi_n(x) \frac{\lambda_n}{|\lambda_n|} \Psi_n^\dagger(y). \quad (6.4)$$

Assuming that all modes with $|\lambda| < \lambda_c/2$ satisfy inequality (4.1) one has

$$|\hat{\gamma}_5^<(x, y)| \leq c_1 a^4 \sum_{|\lambda_n| < \lambda_c/2} \frac{1}{l_n^4} \exp\left(-\frac{|x - x_n^0| + |y - x_n^0|}{2l_n}\right). \quad (6.5)$$

Performing the ensemble average as in previous sections (see in particular Eqs. (3.6) and (4.14)) we find

$$\langle |\hat{\gamma}_5^<(x, y)| \rangle \leq c_1 a^4 \int_a^\infty dl \int_{-\lambda_c/2}^{\lambda_c/2} d\lambda \rho_l'(\lambda) K(|x - y|/l), \quad (6.6)$$

where

$$K(|x - y|/l) = l^{-4} \int d^4 x_0 e^{-(|x-x_0|+|y-x_0|)/(2l)} \approx \frac{|x - y|}{l} e^{-|x-y|/(2l)}. \quad (6.7)$$

The last approximate equality holds for $|x - y| \gg l$, where the integral is dominated by localized modes supported inside a tube of radius l around the straight line connecting x and y . We now invoke the assumption that $l_n \leq l_{max}$ for all $-\lambda_c/2 < \lambda_n < \lambda_c/2$. The “worst-case scenario” is that the l -integral in Eq. (6.6) will be dominated by $l \lesssim l_{max}$. In this case we find the bound

$$\langle |\hat{\gamma}_5^<(x, y)| \rangle \lesssim \exp(-|x - y|/(2l_{max})), \quad (6.8)$$

where constants and power corrections have been ignored. Hence $\hat{\gamma}_5^<$ is local.

The operator $\hat{\gamma}_5^>$ lives in the orthogonal subspace, whose projection operator is $\mathcal{P}_>(x, y) \equiv \delta_{x,y} - \mathcal{P}_<(x, y)$. Here

$$\mathcal{P}_<(x, y) = a^4 \sum_{|\lambda_n| < \lambda_c/2} \Psi_n(x) \Psi_n^\dagger(y) = (\hat{\gamma}_5^<)^2, \quad (6.9)$$

is the projector on the eigenstates with $|\lambda| < \lambda_c/2$. The bound (6.5) evidently applies to $\mathcal{P}_<(x, y)$ as well. Therefore $\mathcal{P}_<$ is local, and, hence, also $\mathcal{P}_>$ is local. Proceeding exactly as in Ref. [36] we write

$$\hat{\gamma}_5^> = H(m_0) |H(m_0)|^{-1} \mathcal{P}_>. \quad (6.10)$$

(Strictly speaking, the right-hand side is defined via its mode expansion.) The expansion of (the eigenvalues of) $|H(m_0)|^{-1}$ in terms of Legendre polynomials may now be invoked, and the locality of $\hat{\gamma}_5^>$ follows.

Let us discuss some implications of this result. In principle one can envisage two extreme situations. If $l_{max} \ll \lambda_c^{-1}$ then the non-locality of $\hat{\gamma}_5^<$ and $\mathcal{P}_>$ may be neglected. The localization range of the overlap will be governed by the mobility edge λ_c , and will be of order λ_c^{-1} . In other words, in the absence of an admissibility constraint, λ_c^2 plays the role of the lower bound on the spectrum of $H^2(m_0)$. The

opposite extreme is that $l_{max} \gg \lambda_c^{-1}$, where we expect the localization range of the overlap to coincide with l_{max} .

In our argument, we did not attempt to maintain the same level of rigor as in Ref. [36]. The advantage of our more heuristic argument is that it deals with the more realistic case of a *density* of localized near-zero modes where the methods of Ref. [36] are inapplicable. Our analysis is only semi-realistic because, in principle, there will be a very tiny, but non-zero probability to encounter an exponentially localized near-zero eigenmode with an arbitrarily large localization length (in a large enough volume). In practice, however, we expect that our assumption of the existence of a finite, not too large l_{max} will be valid for most simulations. Of course, the most important question in any given simulation is how the scale of the typical localization length as well as the size of the mobility edge compare quantitatively to the scale of the physics one is trying to compute.

We now turn to domain-wall fermions with finite N_s . A useful measure of chiral symmetry breaking is the so-called residual mass m_{res} [41], which is essentially the ratio of the two correlators on the right-hand side of Eq. (6.2). Denoting the (euclidean) time coordinate by τ we define

$$m_{res}(\tau, N_s) = \frac{\sum_{\vec{x}} \langle J_{5q}^+(\vec{x}, \tau) J_5^-(\vec{0}, 0) \rangle}{\sum_{\vec{x}} \langle J_5^+(\vec{x}, \tau) J_5^-(\vec{0}, 0) \rangle}, \quad (6.11)$$

where for convenience we have switched to flavor-changing densities. (In terms of the “isospin” symmetry of the two flavors occurring in these densities, the \pm superscripts correspond to the operators τ_{\pm} of Eq. (2.5).)

The study of m_{res} consists of two steps. First, using the transfer matrix formalism of Ref. [3] we derive expressions for the correlators in a fixed gauge-field background. For the numerator in Eq. (6.11) this step is outlined in Appendix B. Next we have to carry out the integration over the gauge field. In general this is quite complicated, and so we will restrict ourselves to two relatively simple cases. Observing that τ is a measure of the four-dimensional separation in Eq. (6.11), we will discuss the τ dependence for fixed $N_s \gg 1$, and the N_s dependence for fixed $|\tau| \gg a$. As before, well inside the C phase we expect the mobility edge of $H(-M, a_5)$ to be a quantity of order one in lattice units. For $\tau = O(a)$ and $N_s \gg 1$, m_{res} will be dominated by the exponentially localized near-zero modes, whereas for $N_s = O(1)$ and $|\tau| \gg a$ it will be dominated by the extended states close to the mobility edge.

The crucial observation is that, as explained earlier, the quark and anti-quark operators of the pseudo-scalar density $J_5^-(\vec{0}, 0)$ live on the two boundaries of the fifth dimension, whereas $J_{5q}^+(\vec{x}, \tau)$ is located midway between the two boundaries. In a diagrammatic language, the fermion (anti-fermion) at the boundary must be connected by a fermion line to the “midway” anti-fermion (fermion). In Eq. (B.1), these two fermion lines come from the one-particle sector of the second-quantized transfer matrix that acts $N_s/2$ times on the fermion (or anti-fermion) at the boundary. The contribution of each mode to a fermion line involves a factor of $\Psi_n(\vec{0}, 0) q_n^{N_s/2} \Psi_n^\dagger(\vec{x}, \tau)$, or its hermitian conjugate.

For $|\tau| \gtrsim a$ the denominator in Eq. (6.11) will contain short-distance contributions

which are of no interest to us. In this case it is simpler to consider the numerator alone. Assuming some fixed $N_s \gg 1$, the contribution of all extended modes has died out, because for them, $q_n^{N_s/2} \lesssim q_c^{N_s/2} \ll 1$. We are left with the contribution of the exponentially localized modes of $H(-M, a_5)$, of which the near-zero modes dominate for $N_s \gg 1$. Following closely the overlap case, Eq. (4.1) allows us to put a bound on $\Psi_n(\vec{0}, 0) \Psi_n^\dagger(\vec{x}, \tau)$. A similar bound applies to the contribution of the second fermion line. The product of the two bounds gives rise to the same exponential factor as on the right-hand side of Eq. (6.5), except that the factor of 1/2 inside the exponent is missing. As before we now assume the existence of a maximal localization length for the near-zero modes, arriving at

$$\sum_{\vec{x}} \langle J_{5q}^+(\vec{x}, \tau) J_5^-(\vec{0}, 0) \rangle \sim \exp(-|\tau|/l_{max}), \quad N_s \gg 1. \quad (6.12)$$

The evident analogy with Eq. (6.8) is not surprising.

Finally, we consider the N_s dependence for $|\tau| \gg a$. Returning to m_{res} , now all the exponentially-localized modes may be neglected. We expect that m_{res} will be dominated by the extended modes of the transfer matrix with eigenvalues close to the mobility edge. The anticipated result is

$$m_{res} \sim q_c^{N_s}, \quad |\tau| \gg a. \quad (6.13)$$

This reflects a cancellation of the τ dependence between the numerator and the denominator in Eq. (6.11), for large τ separations (for numerical evidence supporting this, see Ref. [41]). We are unable to derive this result analytically. We will give a heuristic argument, based on an analogy with perturbation theory, which supports this result.

In perturbation theory, this result is obtained as follows [38]. When the quark mass is zero, the one-loop domain-wall fermion propagator has, near each boundary, a factorizable form. Assuming for definiteness that the right-handed quark resides near the $s = 0$ boundary, the propagator in the vicinity of this boundary is

$$G(x, y; s, s') \approx \chi(s) P_R G(x, y) \chi^\dagger(s'). \quad (6.14)$$

Here $P_R = \frac{1}{2}(1 + \gamma_5)$, x, y are the usual four-dimensional coordinates, and s, s' are coordinates in the fifth dimension. The separation $|x - y|$ is assumed to be large compared to the lattice scale (but small enough for weak-coupling perturbation theory to be applicable). $G(x, y)$ is the effective quark propagator whose tree-level Fourier transform is $1/\not{p}$ for small p , and which, at higher orders, contains the familiar logarithmic self-energy corrections of a massless quark. The s -coordinate wave function $\chi(s)$ carries no Dirac indices.

For an optimally-chosen M as a function of g_0 , the (tadpole-improved) tree-level wave function $\chi_0(s)$ is completely confined to the boundary layer $s = 0$. For $s \geq 1$, the wave function arises from a short-distance, one-loop *quantum* effect. Explicitly, $\chi(s) = \chi_0(s) + g_0^2 \chi_{quantum}(s)$ where $\chi_0(s) = \delta_{s,0}$ and $\chi_{quantum}(s) \sim q_0^s$ up to a power correction. This form of $\chi_{quantum}(s)$ gives rise to Eq. (6.13), with $q_c \rightarrow q_0$. (Since q_0 is

the band edge of the free transfer matrix,¹⁴ the shape of the leading-order $\chi_{quantum}(s)$ depends on the free domain-wall fermion action only. In higher orders one expects $\chi_{quantum}(s) \sim (q_0 f(g_0))^s$ where $f(g_0) = 1 + O(g_0^2)$, and where $f(g_0)$ depends on the gauge action too.)

Restoring the momentum dependence, the s -coordinate wave function $\chi(s; p)$ is universal in the sense that corrections to $\chi(s) = \chi(s; 0)$ vanish like $(ap)^2$. The physical reason is that the propagation in the fifth direction is dominated by a small region in the Brillouin zone surrounding the critical momenta that saturate the band edge q_0 . These momenta are $O(1/a)$. Fluctuations of the gauge field allow low-momentum modes to couple to these lattice-scale modes, with an amplitude that can be naturally expanded in powers of $(ap)^2$. Eq. (6.14) is obtained by keeping only the leading term in this expansion. For all other terms, the $1/\not{p}$ singularity of the (free) propagator is wiped out, and so their effect is negligible for large space-time separations.

Non-perturbatively, we may envisage a similar factorization of the domain-wall fermion propagator for $|\tau| \gg a$ (in a fixed gauge). Again, the extended states close to the mobility edge of the transfer matrix will mediate the s -propagation. Again these extended states will be controlled by the lattice scale, and it is reasonable that their coupling to low-momentum external states will have a universal value. Turning to the correlators of the gauge-invariant pseudo-scalar densities, a factorizable form of the (fixed-gauge) domain-wall fermion propagator, as in Eq. (6.14), implies that the common τ dependence of the numerator and the denominator of Eq. (6.11) is $\exp(-|\tau|m_\pi)$. The result is Eq. (6.13).¹⁵

7. Conclusions

Let us summarize our conclusions and make some additional comments. We start with what we learned about the quenched phase diagram.

In finite volume, we argued that the Aoki condensate is non-zero everywhere in the super-critical region of the phase diagram, and that the pion two-point function always has a $1/m_1$ divergence. This $1/m_1$ divergence arises mainly from exponentially localized near-zero modes. If the restricted spectral density $\rho_l(0)$ is non-zero for some localization length l , then the momentum-space pion two-point function $\tilde{\Gamma}(p)$ exhibits the $1/m_1$ divergence for all momenta up to $p^2 l^2 \sim 1$. Because of this divergence, clearly the finite-volume quenched theory is only well defined with a non-vanishing twisted mass m_1 .

Extending this to infinite volume, we argued moreover that if all near-zero modes are localized, the condensate is approximately equal to $\lim_{m_1 \rightarrow 0} 2m_1 \tilde{\Gamma}(p)$, and the difference vanishes with p^2 . This implies that there are no Goldstone excitations.

Adopting the mobility-edge hypothesis we arrive at the following physical picture. In the super-critical quenched theory the pionic condensate is always non-zero.

¹⁴In Ref. [38], the band edge of the free transfer matrix was denoted q_1 (and not q_0).

¹⁵For the DBW2 gauge action at quenched $a^{-1} \sim 2$ GeV it was found that $q_c \sim 0.6$ [42]. This is very close to the value $q_0 = 0.5$ found in one-loop perturbation theory [38]. Therefore, in this case both higher-order effects and non-perturbative effects are small.

Goldstone poles exist, however, only in part of the super-critical region which, by definition, is the quenched Aoki phase. Inside the Aoki phase the mobility edge vanishes, all the near-zero modes are extended, and the pion two-point function has no $1/m_1$ divergence, because the contribution of extended modes to this divergence goes to zero in the infinite-volume limit. Outside of the Aoki phase the mobility edge is larger than zero, and all the near-zero modes are exponentially localized. There are no Goldstone poles, and the Ward identity (2.9) is saturated instead by the $1/m_1$ divergence of the pion two-point function.

We can, in fact, completely characterize the quenched phase diagram using *two* local order parameters. For the SU(2)-orientation of the twisted-mass term in the action (2.3), one order parameter is the usual condensate $\langle \pi_3 \rangle = 2\pi\rho(0)$. The other is ξ , defined in Eq. (4.10), which measures the size of the $1/m_1$ divergence in the pion two-point function. In the quenched theory $\langle \pi_3 \rangle \neq 0$, and SU(2) is spontaneously broken, in the entire super-critical region. Hence the lines $m_0 = 0$ and $am_0 = -8$ are phase boundaries in the quenched theory. Inside the super-critical region we have a phase with Goldstone bosons (the Aoki phase), and phases with no Goldstone bosons (the C phases, and the super-critical parts of the A regions, which form separate phases in the quenched theory). The order parameter for having *no* Goldstone excitations is $\xi > 0$.

In continuum, infinite-volume, quenched chiral perturbation theory, it is known that the usual condensate $\langle \bar{\psi}\psi \rangle$ develops a $\log(m)$, or $m^{-\delta}$ with δ small, divergence in the limit $m \rightarrow 0$ [8, 43]. In the continuum limit of the lattice theory chiral symmetry is restored, and the Aoki condensate can be rotated back to the usual condensate (see for example Ref. [12]). Turning this argument around, one expects a $\log(m_1)$ divergence of the Aoki condensate inside the Aoki phase in the continuum limit, with $O(am_1)$ corrections due to a non-zero lattice spacing. As explained above, we expect no $1/m_1$ divergence of the pion two-point function inside the Aoki phase in the infinite-volume limit.

In unquenched QCD we do not have any new results. We did verify that, *only* in unquenched QCD, one can prove that the pion two-point function $\tilde{\Gamma}(p)$ is bounded. In finite volume this is always true, while in infinite volume this is true provided $p \neq 0$. Thus, our new results for the quenched theory do not contradict any of the well-known facts for the unquenched case.

The main differences between unquenched and quenched QCD are as follows. Inside the Aoki phase, the differences are accounted for by the chiral lagrangian, and the quenched theory is known to have enhanced chiral logarithms. Outside the Aoki phase, both unquenched and quenched QCD have exponentially localized near-zero modes; in the infinite-volume limit, zero is not an isolated eigenvalue of any gauge-field configuration drawn according to the Boltzmann weight. However, in the quenched theory $\rho(0) \neq 0$, whereas in the full theory $\rho(0) = 0$. Heuristically, this can be understood as follows. Let us compare two infinite-volume gauge-field configurations, which differ only inside a small region whose radius is $O(1)$ in lattice units. Assume that, inside this small region, each configuration supports an exponentially localized mode, with possibly different eigenvalues. In the quenched theory,

these two configurations can have similar Boltzmann weights; but in the unquenched two-flavor theory, each localized mode will contribute to the Boltzmann weight of the corresponding configuration (and, hence, to the spectral density) a factor of $\lambda^2 + m_1^2$ (*cf.* Eq. (2.4)). Therefore the configuration with the smaller eigenvalue will be suppressed. In the limit $m_1 \rightarrow 0$, a configuration supporting an exponentially localized zero mode is completely suppressed in full QCD. In this argument, it is important that the difference between the two configurations is confined to a small region. If all the near-zero modes are extended, a local change in the configuration will have only an infinitesimal effect on any one of the eigenvalues, and the entropy may be large enough to overcome the suppression factor due to the fermion determinant. Thus, the extended modes may still build up a condensate, despite the suppression by the fermion determinant.

On the basis of our analysis, we argued that the domain-wall and overlap formulations work only inside the C phase(s).¹⁶ Inside those phases the mobility edge is non-zero, and all the near-zero modes of the Wilson kernel are exponentially localized. The overlap should be local, and for domain-wall fermions, chiral symmetry should be recovered exponentially with the size of the fifth dimension. Also, the effective four-dimensional overlap operator emerging in the $N_s \rightarrow \infty$ limit (which in the $a_5 \rightarrow 0$ limit coincides with the standard overlap constructed with a Wilson-fermion kernel) should be local. Inside the Aoki phase one encounters infinitely many light unphysical modes, which contribute to the logarithm of the partition function with opposite signs. The overlap operator corresponds to the special case $a_5 \rightarrow 0$. It is hard to imagine how either formulation could remain valid under these circumstances.¹⁷

It is worth commenting on the role of the gauge action in this respect. In particular, let us discuss how precisely an admissibility condition [36] would change the picture. An admissibility condition means that all the plaquette variables are constrained to be closer to one than some $0 < \epsilon \ll 1$. The spectrum of $H^2(m_0)$ then has a lower bound $(\lambda_{min}^0)^2 - \delta^2$ (again λ_{min}^0 refers to the free hamiltonian $H_0(m_0)$), where δ is determined in terms of ϵ . This prevents the existence of near-zero modes when $\lambda_{min}^0 > \delta$, but not when $\lambda_{min}^0 < \delta$. The super-critical region will now be defined as that region in which $H(m_0)$ has zero modes when restricted to gauge fields satisfying the admissibility condition. This new super-critical region consists of five (disconnected) vertical strips in the phase diagram, each of which is located near one of the five critical value of m_0 . Inside each of those super-critical strips there should still be an Aoki phase.

It is clear that, in principle, an admissibility condition guarantees the locality of the (ordinary or generalized) overlap, and the exponential recovery with N_s of the domain-wall's chiral symmetry, for m_0 not close to a critical value. However, imposing an admissibility condition in numerical simulations is prohibitively expensive. Very

¹⁶One quark field per one lattice-fermion field is obtained by taking the continuum limit inside the C phase that borders on the interval $-2 < am_0 < 0$ on the $g_0 = 0$ axis (where $M = -m_0$ is the domain-wall height, and provided $a_5 \leq 1$ [33]). A possible trajectory for taking the continuum limit is indicated by the dashed line in Fig. 1.

¹⁷For other work pointing at difficulties at strong coupling, see Ref. [44]. For related work on the phase structure of overlap fermions with a small hopping parameter, see Ref. [45].

similar results can however be achieved by modifying the lattice gauge and/or fermion action, such that the density of the localized near-zero modes of $H(m_0)$ decreases for a fixed value of the lattice spacing. The density of near-zero modes was studied directly and indirectly in numerous publications; for recent reviews see Ref. [46]. In an approximation where all the exponentially localized modes are neglected, the mobility edge turns into a gap, which can be studied in perturbation theory [38] (see also Ref. [26]). Non-perturbatively, numerical results with the Iwasaki [47] and DBW2 [42] gauge actions show a dramatic depletion of near-zero modes. This likely corresponds to larger values for the mobility edge at fixed lattice spacing. If we would replace the vertical axis in Fig. 1 by the lattice spacing (in physical units) this would amount to a recess of the Aoki-phase boundaries towards larger a , *i.e.* to enlarged C phases.

We have studied the PCAC (Partially-Conserved Axial Current) relation for domain-wall fermions, Eq. (6.2). The residual mass defined in Eq. (6.11) directly provides information on the rate of chiral symmetry restoration as a function of N_s . We argued that, by monitoring the anomalous term in the domain-wall PCAC relation, one can determine *two* crucial features of the “hamiltonian” $H(-M, a_5)$ that controls the propagation in the s -direction: the mobility edge λ'_c (equivalently q_c), *cf.* Eq. (6.13), and (in effect) the average localization length \bar{l} of the near-zero modes, *cf.* Eq. (6.12). These results may be combined as

$$m_{res} \sim \frac{e^{-|\tau|/\bar{l}}}{f(\tau)} + c q_c^{N_s}, \quad (7.1)$$

where c is a constant. (Here we have traded the maximal localization length l_{max} of the near-zero modes, assumed in Sect. 6, by an average localization length \bar{l} .) The function $f(\tau)$ contains the τ dependence of the domain-wall’s pion two-point function in the denominator in Eq. (6.11).¹⁸ This result should be valid provided $N_s \gg 1$ and/or $|\tau| \gg a$.

The residual mass has been extensively studied in domain-wall fermion simulations which according to our terminology correspond to the range $|\tau| \gg a$.¹⁹ As a function of N_s , the results for the Wilson gauge action at quenched $\beta = 6.0$ and optimally chosen M [41] are characterized by a rapid initial drop of m_{res} . However, for larger values of N_s the fall-off slows down, and eventually m_{res} settles at a non-zero value. Therefore, the first term on the right-hand side of Eq. (7.1) is non-negligible in these simulations. According to our physical picture, this suggests that both the density of near-zero modes and their average localization length may be relatively large; hence, in this case, one is very close to the Aoki phase.²⁰ In contrast, the

¹⁸As explained in sect. 6, for $|\tau| \gtrsim a$ Eq. (7.1) is not directly amenable to numerical tests because of the unknown short-distance effects in the pion two-point function; it may be advantageous to study to numerator of Eq. (6.11) directly, *cf.* Eq. (6.12).

¹⁹The simulations often show a nice plateau $m_{res}(\tau, N_s) \approx m_{res}(N_s)$ for a wide range of τ .

²⁰We believe that the first exploratory finite-temperature domain-wall simulations [48] were in fact carried out inside the Aoki phase, which would explain the poor chiral symmetry observed even at relatively large N_s . This is why, in Fig. 1, we have drawn the region where domain-wall simulations have been tried such that it partially overlaps with the Aoki phase.

Iwasaki [47] and DBW2 [42] results exhibit a clean exponential fall-off for all values of N_s where data are available. This implies that the effect of exponentially localized near-zero modes vanishes within numerical accuracy. In these cases the density of near-zero modes should be very small, and their average localization length should be of order one in lattice units; hence one is well outside the Aoki phase.

The “hamiltonian” $H(-M, a_5)$ also serves as a kernel of the generalized overlap operator obtained in the $N_s \rightarrow \infty$ limit, and λ'_c and \bar{l} are the two quantities which control the locality of this operator. The small but non-zero value of m_{res} , found using the Wilson gauge action at quenched $\beta = 6.0$ when both N_s and the separation are large, suggests that in this case the localization scale of the limiting operator might not be sufficiently small compared to the physical scale of the simulation. In contrast, the Iwasaki and DBW2 results imply a highly localized effective four-dimensional operator.

When overlap fermions are employed, as with domain-wall fermions it is necessary to verify whether locality of the overlap operator is obtained, and whether the localization scale is small compared to the physical length scale. This should become a routine practice in any overlap simulation!

The picture for the phase diagram of QCD with Wilson fermions we painted in this paper is for a good part conjectural. In particular, we did not prove the hypothesis about the mobility edge presented in Sect. 4.2. In addition, some of our more rigorous arguments are based on the assumption that, in the regions where the mobility edge does not vanish, a maximum localization length l_{max} exists. However, we would like to emphasize again that our conjecture appears to be the simplest possible way in which we can understand the collected evidence about the quenched and unquenched phase diagrams, incorporating both numerical [15, 16, 20, 21] and analytical [9, 23, 11, 12, 22] results.

In order to test our proposal for the phase diagram, it would be interesting to study the Ward identity (2.9) numerically, in particular in the quenched two-flavor theory. The second term on the left-hand side should show the $1/m_1$ divergence already in finite volume. A comparison with the pionic condensate will test whether the $1/m_1$ divergence saturates the Ward identity for very small momenta. A study of the dependence of all terms in the Ward identity on the volume should make it possible to see in which region of the phase diagram Goldstone excitations occur in the infinite-volume limit. Obviously, such a numerical study will have to include a twisted mass [24], and no (exceptional) configurations should be discarded. Numerical studies can be extended to study localization lengths of near-zero modes as well as non-zero modes outside the Aoki phase, once the location of the various regions in Fig. 1 has been established. The localization length of non-zero modes would yield information on the value of the mobility edge. (As explained earlier, similar information may be obtained from (quenched) domain-wall fermion simulations.) Similar studies can also be done in the unquenched theory, but in that case the spectral density of the localized modes will depend in a more complicated manner on the randomness of the gauge field because of the back-reaction through the fermion determinant. It is interesting that the quenched theory provides a conceptually simpler arena to test the validity of our conjecture!

Acknowledgements

The topics of this work were addressed in the RIKEN BNL Research Center workshop on *Fermion Frontiers in Vector Lattice Gauge Theories*, held on May 6-9, 1998, at Brookhaven National Lab., and more recently in the program *Lattice QCD and Hadron Phenomenology*, held during September - December 2001 at the Institute for Nuclear Theory at the University of Washington, Seattle. We thank the participants for extensive discussions which motivated this work. YS also thanks Amnon Aharony, Ora Entin-Wohlman and Ben Svetitsky for discussions. This research is supported by the Israel Science Foundation under grant 222/02-1. MG is supported in part by the US Department of Energy.

Appendix A

In this Appendix, we consider the issue of localization from a somewhat different angle. Instead of using our criterion for localization of individual eigenmodes, Eq. (4.1), we use Anderson's criterion of (partial) absence of diffusion [27]. The argument reviewed here is originally due to Ref. [49], see also Ref. [28].

In the language of condensed matter, the hermitian Wilson-Dirac operator $H = H(m_0)$ is a "tight-binding" hamiltonian. This means that the "electrons" can reside only on the sites of a regular lattice. This hamiltonian lives in four space dimensions, with coordinates x or y , and determines the evolution of the system in a (fifth, continuous) time dimension, with coordinate s . We will assume that the electron encounters a random potential on each lattice site, defined by some probability distribution. Since there is no back reaction of the electrons on the random potential, this situation corresponds to the quenched approximation of QCD, where of course the gauge fields provide the random potential. We introduce the advanced Green function $\mathcal{G}(x, y; s)$ and its Fourier transform $\mathcal{G}(x, y; \lambda)$

$$\begin{aligned}\mathcal{G}(x, y; s) &= \theta(s) \sum_n \Psi_n(x) \Psi_n^\dagger(y) e^{-i\lambda_n s}, \\ \mathcal{G}(x, y; \lambda) &= \sum_n \Psi_n(x) \Psi_n^\dagger(y) (\lambda - \lambda_n)^{-1},\end{aligned}\tag{A.1}$$

which solve the equations

$$\begin{aligned}(i\partial/\partial s - H)\mathcal{G}(x, y; s) &= i\delta^4(x - y)\delta(s), \\ (\lambda - H)\mathcal{G}(x, y; \lambda) &= \delta^4(x - y).\end{aligned}\tag{A.2}$$

To carry out the Fourier transform, λ has to be in the upper half plane, whereas taking it in the lower half plane corresponds to $\mathcal{G}(x, y; \lambda)$ being the transform of the retarded Green function.

We now adopt the point of view that the electron is partially localized if there is a non-zero probability for the electron to be found at a specific location y after an arbitrarily long time, given that it started out at some other location x . This probability is given by $\langle |\mathcal{G}(x, y; s)|^2 \rangle$ for $s \rightarrow \infty$, where $\langle \dots \rangle$ denotes the statistical

average over the random potential at each lattice site (or, in the QCD case, at each lattice link). The idea is that this non-zero probability arises from localized states, whereas the probability to escape to infinity comes from extended states. Obviously, in a finite volume there is no clear distinction between these two probabilities, but one may study the dependence of $\langle |\mathcal{G}(x, y; s)|^2 \rangle$ for $s \rightarrow \infty$ on the volume. If it stays non-zero in the infinite-volume limit, we have (partial) localization.

Following Ref. [49], we may express the limiting value of $\langle |\mathcal{G}(x, y; s)|^2 \rangle$ in terms of ensemble averages of the Fourier transform $\mathcal{G}(x, y; \lambda)$:

$$\lim_{s \rightarrow \infty} \langle |\mathcal{G}(x, y; s)|^2 \rangle = \lim_{\eta \rightarrow 0} \eta \int_0^\infty ds e^{-\eta s} \langle |\mathcal{G}(x, y; s)|^2 \rangle \quad (\text{A.3})$$

$$= \lim_{\eta \rightarrow 0} \left\langle \sum_{k,n} \Psi_n(x) \Psi_n^\dagger(y) \Psi_k(y) \Psi_k^\dagger(x) \frac{\eta}{\eta + i(\lambda_n - \lambda_k)} \right\rangle \quad (\text{A.4})$$

$$= \lim_{\eta \rightarrow 0} \frac{\eta}{2\pi} \int d\lambda \langle \mathcal{G}(x, y; \lambda + i\eta/2) \mathcal{G}(y, x; \lambda - i\eta/2) \rangle. \quad (\text{A.5})$$

Equality (A.3) follows after a partial integration (after which the limit $\eta \rightarrow 0$ can be taken); the other two follow from elementary integrations. These equations are valid in finite volume, and we will assume that they are valid in infinite volume as well.

We observe that the integrand on the right-hand side of Eq. (A.5) corresponds precisely to Eq. (3.1), *i.e.* the pion two-point function, for $\lambda = 0$ and identifying $\eta/2 = m_1$. With the Anderson criterion for localization, we immediately conclude that the λ -integral of the two-point function has a $1/\eta$ divergence provided $\lim_{s \rightarrow \infty} \langle |\mathcal{G}(x, y; s)|^2 \rangle > 0$. In finite volume this is always the case, whereas in infinite volume, this is the case if the electron is (partially) localized.

Anderson localization implies that, by definition, the probability for the electron *not* to escape to infinity, given by $\lim_{s \rightarrow \infty} \langle |\mathcal{G}(x, y; s)|^2 \rangle$, is non-zero, and thus that

$$\langle \mathcal{G}(x, y; \lambda + i\eta) \mathcal{G}(y, x; \lambda - i\eta) \rangle \propto \eta^{-1}, \quad \eta \rightarrow 0 \quad (\text{A.6})$$

for a range of λ (note that this correlation function is positive). It follows that localization for a given λ may be *defined* as the existence of this divergence [49]. This coincides with our analysis based on the mobility-edge hypothesis: if the mobility edge $\lambda_c > 0$, all modes with $\lambda < \lambda_c$ contribute to the $1/m_1$ (or $1/\eta$) divergence, and thus the right-hand side of Eq. (A.5) does not vanish, leading to a non-zero probability for the electron not to diffuse.

In reality, it may not be easy to measure the limiting value of $\langle |\mathcal{G}(x, y; s)|^2 \rangle$ experimentally, because all the electronic states are filled up to the Fermi energy. The nature of the eigenstates close to the Fermi energy determine the macroscopic properties (at sufficiently low temperature). A disordered system is an insulator (zero electric conductivity) if the electronic states at the Fermi energy are localized, whereas a metallic behavior (non-zero conductivity) is observed if the electronic states at the Fermi energy are extended. A *metal-insulator* phase transition occurs when a mobility edge reaches the Fermi energy. The Aoki phase transition is in this sense a special kind of a metal-insulator transition. For a discussion employing these concepts in the context of the chiral phase transition in continuum QCD, see Ref. [50].

Finally, we mention that the concept of an effective lagrangian for the long-range degrees of freedom which is used to study the phase diagram of lattice QCD [12, 22], is also widely used in condensed-matter disordered systems, see Refs. [29, 30] and references therein.

Appendix B

Using the operator formalism and the notation of Ref. [3], the numerator in Eq. (6.11) is a sum of four positive terms. For a fixed gauge field (and in an arbitrary normalization) one of these terms is

$$\langle 0' | \hat{c}_\downarrow(\vec{0}, 0) \hat{T}^{N_s/2} \hat{c}_\downarrow^\dagger(\vec{x}, \tau) \hat{c}_\uparrow(\vec{x}, \tau) \hat{T}^{N_s/2} \hat{c}_\uparrow^\dagger(\vec{0}, 0) | 0' \rangle. \quad (\text{B.1})$$

Here \hat{T} is the second-quantized transfer matrix. \hat{c}^\dagger and \hat{c} are fermion creation and annihilation operators. The up and down arrows represent two different flavors. Spin indices have been suppressed. The state $|0'\rangle$ is a reference state annihilated by all the \hat{c} 's. It encodes the boundary conditions in the fifth dimension. (For notational simplicity we have given the result when the quark mass is zero; all arguments generalize to the case of a non-zero mass, as well as to the other three terms that we do not show.)

The composite operator $\hat{c}_\downarrow^\dagger(\vec{x}, \tau) \hat{c}_\uparrow(\vec{x}, \tau)$ belongs to the pseudo-scalar density $J_{5q}^\pm(\vec{x}, \tau)$ located in the middle of the five-dimensional bulk. Therefore, to be reached from one of the boundaries, one has to act $N_s/2$ times with the transfer matrix (we assume that N_s is even). If an admissibility condition is imposed, the (first-quantized) transfer matrix $T(M, a_5)$ has a gap (*i.e.* there are no eigenvalues in some open neighborhood of one). In the limit $N_s \rightarrow \infty$, $\hat{T}^{N_s/2}$ becomes proportional to the ground-state projector $|0_H\rangle \langle 0_H|$. (The ground state $|0_H\rangle$ of \hat{T} is obtained by filling the Dirac sea of states that correspond to all eigenvalues $\omega_n > 1$ of $T(M, a_5)$.) In this case expression (B.1) is proportional to $\langle 0_H | \hat{c}_\downarrow^\dagger(\vec{x}, \tau) \hat{c}_\uparrow(\vec{x}, \tau) | 0_H \rangle$, which is in fact identically zero, because the (in general non-zero) states $\hat{c}_\uparrow | 0_H \rangle$ and $\hat{c}_\downarrow | 0_H \rangle$ have different flavors and, hence, are orthogonal. Thus, the numerator in Eq. (6.11) vanishes and chiral symmetry is recovered (exponentially) in the limit $N_s \rightarrow \infty$. The case of realistic gauge actions is discussed in Sect. 6.

References

- [1] K. Wilson, in *New Phenomena in Sub-Nuclear Physics* (Erice, 1975), ed. A. Zichichi (Plenum, New York, 1977)
- [2] D. B. Kaplan, Phys. Lett. **B288** (1992) 342 [hep-lat/9206013]; Y. Shamir, Nucl. Phys. **B406** (1993) 90 [hep-lat/9303005]
- [3] V. Furman and Y. Shamir, Nucl. Phys. **B439** (1995) 54 [hep-lat/9405004]

- [4] R. Narayanan and H. Neuberger, Phys. Lett. **B302** (1993) 62 [hep-lat/9212019]; Nucl. Phys. **B412** (1994) 574 [hep-lat/9307006]; Nucl. Phys. **B443** (1995) 305 [hep-th/9411108]
- [5] H. Neuberger, Phys. Lett. **B417** (1998) 141 [hep-lat/9707022]
- [6] P.H. Ginsparg, K.G. Wilson, Phys. Rev. **D25** (1982) 2649 M. Lüscher, Phys. Lett. **B428** (1998) 342 [hep-lat/9802011]
- [7] A. Morel, J. Physique **48** (1987) 111
- [8] C. Bernard and M. Golterman, Phys. Rev. **D46** (1992) 853 [hep-lat/9204007]
- [9] S. Aoki, Phys. Rev. **D30** (1984) 2653; **33** (1986) 2399; **34** (1986) 3170; Phys. Rev. Lett. **57** (1986) 3136; Nucl. Phys. B (Proc. Suppl.) **60A** (1998) 206 [hep-lat/9707020]
- [10] A. Casher, Phys. Lett. **B83** (1979) 395; T. Banks and A. Casher, Nucl. Phys. **B169** (1980) 103
- [11] M. Creutz, Phys. Rev. **D52** (1995) 2951; Rev. Mod. Phys. **73** (2001) 119 [hep-lat/0007032]
- [12] S. Sharpe and R. Singleton, Phys. Rev. **D58** (1998) 074501 [hep-lat/9804028]
- [13] R. Kenna and J.C. Sexton, Phys. Rev. **D65** (2002) 014507
- [14] N. Kawamoto and J. Smit, Nucl. Phys. **B192** (1981) 100
- [15] S. Aoki and A. Gocksch, Phys. Lett. **B231** (1989) 449; **B243** (1990) 409; Phys. Rev. **D45** (1992) 3845; S. Aoki, T. Kaneda and A. Ukawa, Phys. Rev. **D56** (1997) 1808 [hep-lat/9612019]
- [16] S. Aoki, A. Ukawa and T. Umemura, Phys. Rev. Lett. **76** (1996) 873 [hep-lat/9508008]; Nucl. Phys. B (Proc. Suppl.) **47** (1996) 511 [hep-lat/9510014]; S. Aoki, T. Kaneda, A. Ukawa and T. Umemura, Nucl. Phys. B (Proc. Suppl.) **53** (1997) 438 [hep-lat/9612010]; K. Bitar, Nucl. Phys. B (Proc. Suppl.) **63** (1998) 829 [hep-lat/9709086]
- [17] M.B. Einhorn and J. Wudka, Phys. Rev. **D67** (2003) 045004 [hep-ph/0205346]
- [18] J. Smit and J. Vink, Nucl. Phys. **B286** (1987) 485
- [19] W. Bardeen, A. Duncan, E. Eichten, G. Hockney and H. Thacker, Phys. Rev. **D57** (1998) 1633 [hep-lat/9705008]; W. Bardeen, A. Duncan, E. Eichten and H. Thacker, Phys. Rev. **D59** (1999) 014507 [hep-lat/9806002]
- [20] R.G. Edwards, U.M. Heller and R. Narayanan, Nucl. Phys. **B522** (1998) 285 [hep-lat/9801015]; Nucl. Phys. **B535** (1998) 403 [hep-lat/9802016]; Phys. Rev. **D60** (1999) 034502 [hep-lat/9901015]

- [21] K. Jansen, C. Liu, H. Simma and D. Smith, Nucl. Phys. B (Proc. Suppl.) **53** (1997) 262 [hep-lat/9608048]
- [22] M. Golterman, S. Sharpe and R. Singleton, in preparation
- [23] F. Berruto, R. Narayanan and H. Neuberger, Phys. Lett. **B489** (2000) 243 [hep-lat/0006030]
- [24] R. Frezzotti, P.A. Grassi, S. Sint and P. Weisz, JHEP **0108** (2001) 058 [hep-lat/0101001]; R. Frezzotti, hep-lat/0210007
- [25] A.J. McKane and M. Stone, Ann. Phys. **131** (1981) 36
- [26] S. Aoki and Y. Taniguchi, Phys. Rev. **D65** (2002) 074502 [hep-lat/0109022]; S. Aoki, Nucl. Phys. B (Proc. Suppl.) **109** (2002) 70 [hep-lat/0112006]
- [27] P.W. Anderson, Phys. Rev. **59** (1958) 1492; N.F. Mott, J. Non-Cryst. Solids **1** (1968) 1
- [28] D.J. Thouless, Phys. Rep. **13** (1974) 93
- [29] K.B. Efetov, Adv. Phys. **32** (1983) 53
- [30] B. Kramer and A. MacKinnon, Rep. Prog. Phys. **56** (1993) 1469
- [31] H. Leutwyler and A. Smilga, Phys. Rev. **D46** (1992) 5607
- [32] G.S. Guralnik, C.R. Hagen and T.W.B Kibble, *Broken Symmetries and the Goldstone Theorem*, in R.L. Cool and R.E. Marshak, Eds., *Advances in Particle Physics*, Vol. 2, Wiley, 1968
- [33] Y. Shamir, Phys. Rev. **D59** (1999) 054506 [hep-lat/9807012]
- [34] C. Bernard and M. Golterman, Phys. Rev. **D49** (1994) 486 [hep-lat/9306005]; O. Bär, G. Rupak and N. Shores, hep-lat/0210050
- [35] I. Horvath, Phys. Rev. Lett. **81** (1998) 4063 [hep-lat/9808002]
- [36] P. Hernández, K. Jansen and M. Lüscher, Nucl. Phys. **B552** (1999) 363-378 [hep-lat/9808010]
- [37] S. Aoki, Y. Taniguchi, Phys. Rev. **D59** (1999) 054510 [hep-lat/9711004]; P. Vranas, Phys. Rev. **D57** (1998) 1415 [hep-lat/9705023]; S. Aoki, T. Izubuchi, Y. Kuramashi and Y. Taniguchi, Phys. Rev. **D59** (1999) 094505 [hep-lat/9810020]; S. Aoki and Y. Taniguchi, Phys. Rev. **D59** (1999) 094506 [hep-lat/9811007]
- [38] Y. Shamir, Phys. Rev. **D62** (2000) 054513 [hep-lat/0003024]
- [39] H. Neuberger, Phys. Rev. **D57** (1998) 5417 [hep-lat/9710089]; Y. Kikukawa and T. Noguchi, hep-lat/9902022

- [40] A. Borici, Nucl. Phys. B (Proc. Suppl.) **83** (2000) 771 [hep-lat/9909057]; hep-lat/9912040
- [41] P. Vranas, Phys. Rev. **D57** (1998) 1415 [hep-lat/9705023]; T. Blum and A. Soni, Phys. Rev. Lett. **79** (1997) 3595 [hep-lat/9706023]; T. Blum, Nucl. Phys. B (Proc. Suppl.) **73** (1999) 167 [hep-lat/9810017]; S. Aoki, T. Izubuchi, Y. Kuramashi and Y. Taniguchi, Nucl. Phys. B (Proc. Suppl.) **83-84** (2000) 624 [hep-lat/9909154]; S. Aoki, T. Izubuchi, Y. Kuramashi and Y. Taniguchi, Phys. Rev. **D62** (2000) 094502 [hep-lat/0004003]; T. Blum *et. al.* (RBC collaboration), hep-lat/0007038
- [42] C. Orginos (RBC collaboration) Nucl. Phys. B (Proc. Suppl.) **106** (2002) 721 [hep-lat/0110074]; Y. Aoki *et. al.* (RBC collaboration), hep-lat/0211023
- [43] S. Sharpe, Phys. Rev. **D46** (1992) 3146 [hep-lat/9205020]
- [44] R. C. Brower and B. Svetitsky, Phys. Rev. **D61** (2000) 114511 [hep-lat/9912019]; F. Berruto, R.C. Brower and B. Svetitsky, Phys. Rev. **D64** (2001) 114504 [hep-lat/0105016]
- [45] M. Golterman and Y. Shamir, JHEP **0009** (2000) 006 [hep-lat/0007021]
- [46] P. Hernández, Nucl. Phys. B (Proc. Suppl.) **106** (2002) 80 [hep-lat/0110218]; R.G. Edwards, Nucl. Phys. B (Proc. Suppl.) **106** (2002) 38 [hep-lat/0111009]
- [47] A. Ali Khan *et al.* (CP-PACS collaboration), Phys. Rev. **D63** (2001) 114504 [hep-lat/0007014]
- [48] P. Chen *et. al.*, Phys. Rev. **D64** (2001) 014503 [hep-lat/0006010]; P. Vranas, hep-lat/0001006
- [49] E.N. Economou and M.H. Cohen, Phys. Rev. Lett. **25** (1970) 1445
- [50] R.A. Janik, M.A. Nowak, G. Papp and I. Zahed, Phys. Rev. Lett. **81** (1998) 264 [hep-ph/9803289]; Phys. Lett. **B442** (1998) 300 [hep-ph/9807550]